

Received 19 February 2025; revised 5 April 2025; accepted 12 April 2025. Date of publication 18 April 2025; date of current version 12 August 2025.

Digital Object Identifier 10.1109/OJAP.2025.3562292

Additive Manufacturing of Antennas and RF Components for SATCOM: A Review

HAFSA TALPUR^{ID 1} (Member, IEEE), ULAN MYRZAKHAN¹ (Member, IEEE),
JUAN ANDRES VÁSQUEZ-PERALVO^{ID 1} (Member, IEEE), SHUAI ZHANG^{ID 2} (Fellow, IEEE),
AND SYMEON CHATZINOTAS^{ID 1} (Fellow, IEEE)

¹Interdisciplinary Centre for Security Reliability and Trust, University of Luxembourg, 1855 Luxembourg City, Luxembourg

²Antennas, Propagation and Millimeter-wave Systems Section, Department of Electronic Systems, Aalborg University, 9220 Aalborg, Denmark

CORRESPONDING AUTHOR: H. TALPUR (e-mail: hafsa.talpur@uni.lu).

This work was supported by the Luxembourg National Research Fund (FNR), through the CORE Project (C³): Cosmic Communications Constructions under Grant C23/IS/18116142.

ABSTRACT In the past few years, additive manufacturing (AM) technology has developed into a revolutionary factor in the design and manufacturing of satellite RF/antenna components, providing benefits over traditional manufacturing techniques, such as cost-efficient, lightweight structure, complex design flexibility, and monolithically integrates different parts in signal structure. AM profoundly impacts how satellite antennas, waveguides, and other RF components are manufactured and deployed across several orbital regimes. However, complex atmospheric conditions in space primarily affect satellite system performance, degrading antenna efficiency and longevity. This is due to many reasons, mainly extreme thermal cycle variation, atmospheric radiations, vacuum environment, and mechanical pressure; hence the choice of AM technique and material are crucial for onboard satellite components design to ensure system performance stability. Based on the latest research, this paper provides a review of current state-of-the-art AM printed antennas and RF components incorporating different AM techniques and materials to obtain specific design characteristics such as high gain, wide bandwidth, beamforming, and better power handling capacity, particularly for Ku, K, and Ka-band satellite communication (SATCOM). Furthermore, the paper highlights some techniques to enhance the performance of existing AM technologies and material properties, making them suitable for onboard SATCOM applications that withstand extreme atmospheric conditions. The paper serves as a valuable guide on the AM of SATCOM antenna/RF component design, providing insights into material selection and AM techniques for efficient fabrication.

INDEX TERMS Additive manufacturing, antenna, fused deposition modeling, direct metal laser sintering, radio-frequency (RF) components, satellite communication, sintering laser melting, stereolithography, polyjet.

I. INTRODUCTION

IN THE realm of wireless communication, antennas, metamaterials, metasurface, and radio frequency (RF) components play the important role in transmitting and receiving electromagnetic signals to enable terrestrial and non-terrestrial communication systems [1]. The areas where terrestrial infrastructure is limited or non-existing, satellite communication (SATCOM) provides high-speed and reliable connections resulting in global connectivity, operating critical services such as Internet access, television broadcasting, emergence response etc.

Traditional radiating systems for SATCOM, such as antennas, waveguides, phase shifters, and corresponding feed chain components, have been developed using subtractive manufacturing methods such as molding, milling, or casting [2], [3]. These methods provide precision, ensure exceptional surface finish, and easily design complex structures for stable and efficient performance at high frequencies. But the techniques are expensive, time-consuming, and limited by geometrical constraints like lattice or conformal structures. Some complex structures can be designed using above methods by splitting the structure into several parts,

TABLE 1. Comparison between additive manufacturing & subtractive manufacturing.

Criteria	Additive Manufacturing	Subtractive Manufacturing
Material	Thermoplastic/ Polymer Metals Composites Ceramic	Plastic Metals Composites Ceramic
Material Conductivity	Lower (AM-compatible conductive materials)	High (pure metals used)
Lead time/ Cost	Low	High
Design Flexibility	Ideal for complex design lattice structures	Less design flexibility
Mechanical Strength	Lower (depends on geometry & material used)	High (proven for space use)
Resolution	High resolution (10-50 microns) Low resolution (100-200 microns)	High resolution (\pm 2.5 microns)
Material efficiency	Reduced material waste	High material waste
Post-processing	Required for surface finish and metallization	Not required

which are assembled later by using pins or screws, resulting in a bulky design, and possessing acceptable performance only up to mm-wave frequency. Thus, these conventional fabrication methods cannot produce antenna/RF components that would meet the cost-efficient, and fast manufacturing requirements of modern onboard SATCOM systems because not most of them are inhouse [4].

One transformative approach to SATCOM is the use of AM in the development of antennas and RF components. AM has already emerged in the wireless communication world and gained significant attention in the research communities and industries due to its several advantages such as low cost, rapid prototyping, no mold requirements, compact design, and thus, allowing monolithic integration of designed components with almost no material waste which is high in conventional techniques [5], [6]. Comparison is shown in Table 1. AM mostly use materials such as thermoplastic polymers, ceramics and metal alloys in powdered form to manufacture components which leads to key challenge of ensuring functionality of designed structures in harsh space environment.

Despite significant advancements, only a limited number of investigations have confirmed the performance of AM-based antenna/RF components under the adverse space atmospheric conditions such as extreme thermal cycle, atmospheric radiations, and vacuum environment. Furthermore, the literature still lacks the comprehensive study of identifying the suitable AM technologies and materials for onboard satellite radiating components. Moreover, the selection of materials and AM techniques for SATCOM components must be customized to satisfy certain mechanical, thermal,

and electrical requirements—a topic that has not yet been effectively addressed in the literature.

This article aims to identify above-mentioned gaps by thoroughly reviewing the most recent advancements in AM techniques and materials for the fabrication of antenna/RF components for SATCOM particularly for Ku, K, and Ka bands. It discusses challenges such as minimizing porosity, thermal stability and achieving high resolution and explores innovative technologies like Digital Light Processing (DLP), Direct Laser Writing (DLW) and micro-SLA. The paper also identifies possible preprocessing techniques and material advancements that can be possible used to enhance the component performance for onboard SATCOM. The review is divided into five sections. A detailed introduction of AM technology and its manufacturing process is provided in Section II, with reviewing main techniques used in SATCOM applications. Section III reviews the innovative work from the literature associated to the AM antenna/RF components, showing innovative designs and approaches for minimizing impact of AM on the performance of designed component. This section is further divided according to types of antennas and RF components. Section IV discusses the effect of various space atmospheric challenges on onboard SATCOM components, along with addressing possible advancement in this area to make AM suitable for onboard satellite applications. Finally, main conclusion and future perspective is given in Section V.

II. AM TECHNOLOGIES IN SATELLITE COMMUNICATION

AM technology was initially discussed in 1980s by Hideo Kodama, when he introduced photopolymer material to light and designed a three-dimensional prototype, layer by layer [7]. Later in 1986, Charles Hull invented first AM technique, Stereolithography (SLA), regarded as the first technology for fast prototyping and for his discovery, he filed a patented and become the founder of first commercially available SLA AM technology [8]. After hull's invention, Selective Laser Sintering (SLS) was developed by Carls Deckard in 1988, that uses laser to melt tiny particles of ceramics, plastic, or metals to create objects [8]. A year later, the founder of Stratasys, Scott Crump invented another popular AM technology called Fused Deposition Modeling (FDM) [9]. Now as per American Society for Testing and Materials (ASTM) standard F2792, AM is divided into seven categories based on methods/ process of formation of the product as shown in Fig. 1.

AM techniques have advanced significantly over time, and several technologies are currently in use in many application domains, such as the medical, automotive, and aerospace industries. This growing utilization of AM technology across numerous industries is mainly due to affordable and fast manufacturing. In recent years, AM technology has been widely used in the SATCOM sector, from the development of microwave and mm-wave radiating components like antennas to beamforming networks. The adaptability of AM technology is evident as it effectively addresses the

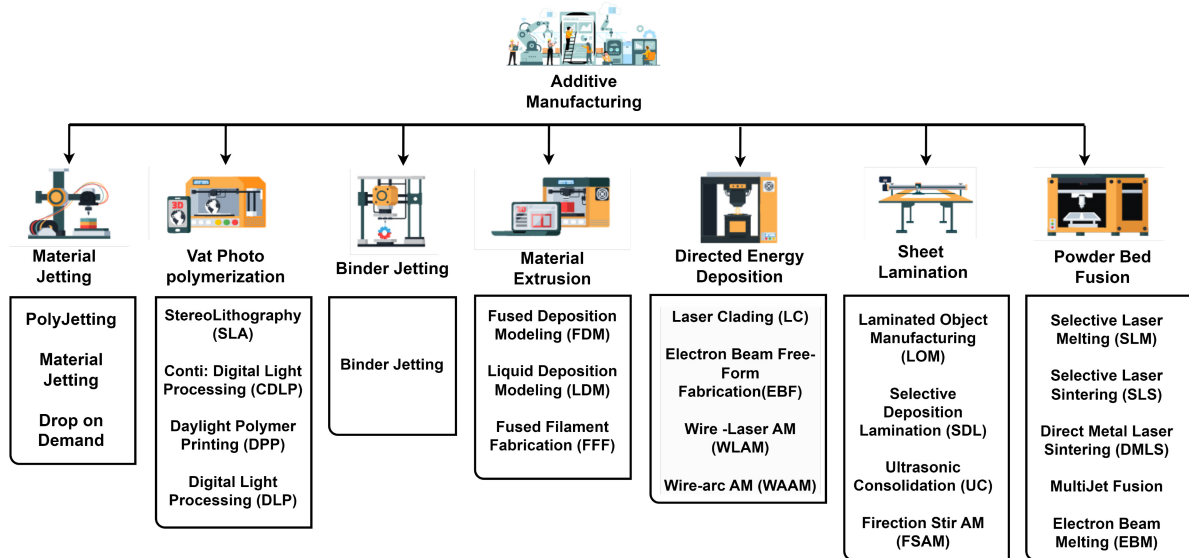


FIGURE 1. Categories of AM technology.

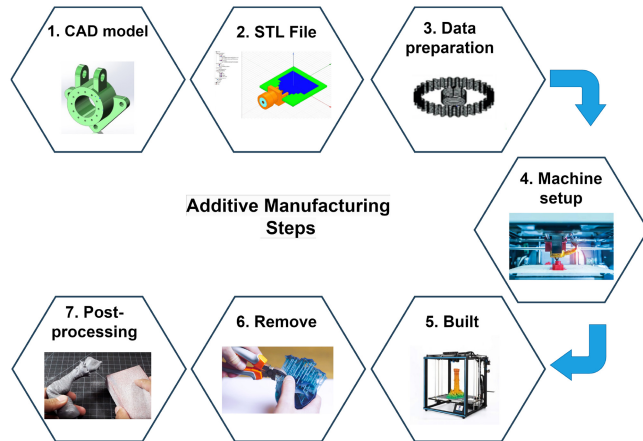


FIGURE 2. Steps of Additive Manufacturing technology.

constantly increasing complexities in SATCOM systems, particularly after adapting higher frequency bands for all types of services.

In generic AM process illustrated in Fig. 2, three-dimensional (3D) model is generated using any Computer Aided Design (CAD) software, it is than converted into STL file format that links 3D model with its approximate lattice structure. Then, STL file is handed over to AM machine for 3D printing [10]. Furthermore, some AM technologies build supporting structure along with the design, which is then removed physically before post-processing.

With regards to onboard SATCOM, our investigation reveals that AM technologies including FDM, SLA, Polyjet and Selective Laser Melting (SLM)/Direct Metal Laser Sintering (DMLS) are widely used techniques. It is important to note that each type of AM technique follows different process to manufacture components shown in Fig. 3. For example, FDM, SLA and Polyjet mostly print dielectric

structures and later perform metallization. They mostly use polymers, due to their advantage of low cost, light weight and easily available. However, at higher frequencies, right choice of metallization process is important for components printed on dielectric structures. On the other side SLM, SLS, and DMLS results in direct metal structure printing [11]. A key consideration in the AM for satellite components is material selection. The atmospheric conditions in space largely effect the performance of onboard satellite antenna/RF components therefore choice of material's parameter should comply with harsh atmospheric conditions in space. The parameters such as thermal resistance, mechanical strength and UV radiation resistance of materials are important to consider while designing satellite radiating components. With respect to SATCOM, these technologies are briefly reviewed in the following subsections.

A. FUSED DEPOSITION MODELING

FDM uses material extrusion technique in which filament is melted inside liquefier chamber using an extrusion channel and positioned on layer in building platform, that layers ultimately result in construction of desired object [13] as shown in Fig. 3. The nozzle diameter determines the precision (about 100-200 μm), resolution, and printing pace of the device, while the liquefier chamber temperature permits maintaining the material in a molten condition without compromising its qualities. For the FDM method, a large variety of thermoplastic materials are accessible [14]. The materials commonly used in FDM are polylactic acid (PLA), acrylonitrile butadiene styrene (ABS), poly carbonate (PC), PEEK and ULTEM. Apart from all these materials, PEEK and ULTEM provide outstanding electrical properties, strength, and stiffness along with high durability [15], [16]. FDM allows multi-material printing in which dielectric and conductive parts of antenna/RF components are printed

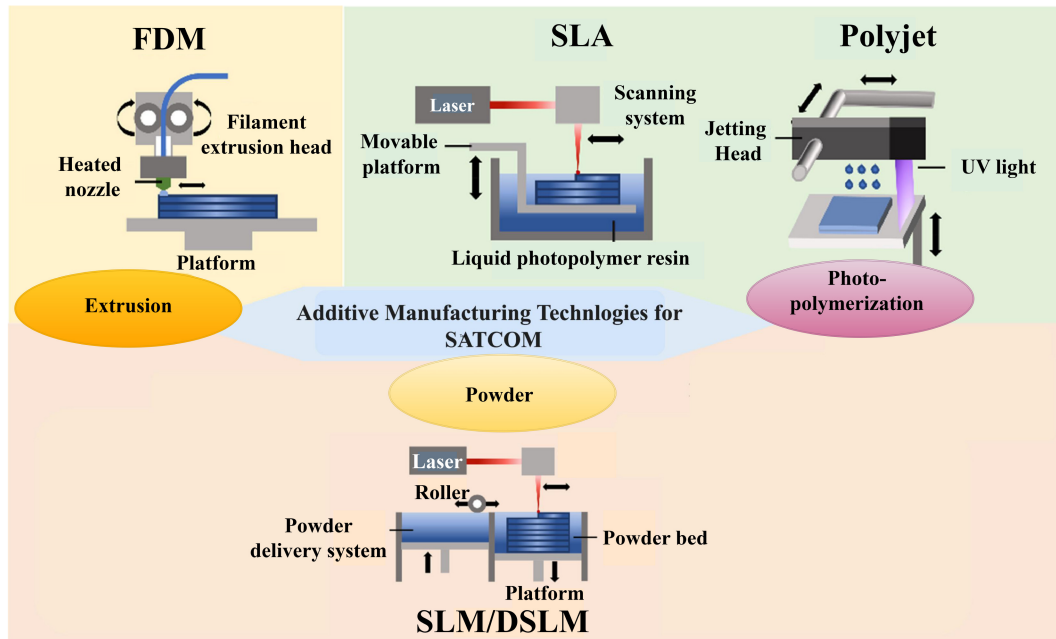


FIGURE 3. Mostly used AM technologies in SATCOM [12].

together in a single process. In recent years, FDM has been considered affordable and suitable AM technology for low-frequency SATCOM applications because, at low frequencies, wavelength increases; therefore, surface finish and structural precision become less critical. It also allows the manufacturing of improved polymers with fillers for stable thermal and mechanical properties, such as Carbon-Fiber reinforced PEEK (CF-PEEK), which is important for onboard SATCOM. FDM also allows the direct printing of conductive structures using conductive filaments in place of polymers to design RF devices. However, the results obtained using these filaments are far worse than those obtained by an antenna designed with the dielectric polymer and copper coating [17].

B. STEREOLITHOGRAPHY

SLA is the first invented AM process. SLA falls under the vat polymerization technique in which a liquid vat of photocurable resin is exposed to a UV laser to solidify the layer, ultimately constructing the solid structure shown in Fig. 3. It involves post-processing steps following washing to clean extra resin, UV curing, extracting supporting structure after printing, and lastly metallization process is carried out, all these steps make manufacturing process time consuming as compared to other AM technologies [13]. It produces optimal miniature components as it has a high resolution of $20\mu\text{m}$ and a surface finish of around $1\mu\text{m}$ or less, which allows high quality and precise fabrication of high frequency SATCOM components [18]. Like FDM, SLA also supports various polymers and ceramic materials. Ceramic SLA is widely used technology in printing dielectric antennas (lens antennas) [19], dielectric resonators (DRA) [20], and

other high-frequency ceramics with low dielectric and energy dissipated losses. It also helps to fabricate high-performance, complex hollow-waveguide structures required in space industry [21].

Additionally, the method uses photopolymer resins (probably added with particles of ceramics) to create lightweight components that are essential for satellites, where mass reduction is paramount. However, these resins have a high coefficient of thermal expansion (CTE) and low thermal conductivity and are brittle by nature. To guarantee their suitability for onboard SATCOM applications, a precise trade-off between the mechanical and thermal characteristics of photopolymer resins and the operating conditions needs to be carefully considered.

C. POLYJET

PolyJet printing falls under material jetting, is an inkjet technology that utilizes polymer to model 3D structure. As illustrated in Fig. 3, it has two inkjet openings: one for structure design and another for building support structure. The jetting nozzles spray photo-resin across X and Y plan layer-by-layer following the CAD design until the structure is complete. Designed sample contains lattice periodic structure which is linked/photopolymerized using ultra-violet (UV) lamp. Their support structure is water soluble, easily detached using hands or solution bath [13], hence it has the ability of fast manufacturing smooth structure with complex design. However, further metallization process is used to incorporate conductor in the antenna/RF component design. Two inkjet nozzles also help to print multi-material or multi-color by extruding different polymers simultaneously enabling the fabrication of components with variable material



properties making it suitable for different onboard SATCOM applications.

Due to its good precision and multi-material property, it can be used in SATCOM industry to design mm-wave and microwave components such as dielectric antennas [22], phased arrays [23], frequency selective surfaces (FSS) [24], and metamaterial structures [25].

D. SELECTIVE LASER MELTING / DIRECT METAL LASER SINTERING

SLM and DMLS technologies both falls under the Laser Powder Bed Fusion (LPBF) technique in which powdered material such as polymer, metal or ceramic are used to design parts. LPBF has the advantage of producing direct metal structure without undergoing any post-processing or metallization process [26] overcoming the challenges such as brittle, low thermal conductivity and high CTE faced by polymer resins in SLA which makes components less efficient for high-power RF onboard SATCOM applications.

In LPBF process, prepossessing of geometry starts soon after the STL model is imported into SLM/DMLS machine, and supporting structures are designed for the hanging parts. After all preprocessing, the powder material is uniformly spread over the platform than exposed to high-power fiber-laser beam which melts or in case of DLSM sinter all the already deposited powder layer as shown in Fig. 3. After melting, particles are combined and solidify to build the part layer. The process is repeated until the whole structure is completed. Following the completion of the SLM/DLSM manufacturing process, the parts are stripped of all remaining powder and put through a high-temperature stress-relieving procedure while still linked to the building platform. The goal of this method is to minimize part deformation brought on by inner stress that developed during the manufacturing process. Following the components' separation from the building platform, the inner surfaces of the components are shot-peened, and the flanges are polished to enhance their surface quality [13]. LPBF ensures high-quality fabrication by operating in an inert environment (such as nitrogen or argon) to stop the metal powder from oxidizing. In LPBF variety of materials such as titanium, stainless steel, nickel alloy, cobalt chrome, and aluminum are employed. Mostly RF components used aluminum alloy AlSi10Mg for fabrication as it has the high strength per unit mass. LPBF provide dimensional accuracy in range of 40-80 μ m with surface roughness around 3-8 μ m. The quality of printed components depends on the print orientation, structure complexity and the machine operator's experience. In SATCOM, LPBF AM technology could be technological solution to fabricate all-metal structured antennas/RF components for microwave and millimeter-wave [27], [28].

III. RECENT STATE-OF-THE-ART IMPLEMENTATION OF AM TECHNOLOGY IN SATELLITE COMMUNICATION

Generally, electronic components involve in radiating system includes antennas, and RF components. To design these components for onboard SATCOM needs majorly two precise

considerations, one is choice of antenna and RF component design, and other choice of material and manufacturing technique because using AM technology with different base materials (polymers, ceramics, or metal powders) will affect the performance of the SATCOM system accordingly. In literature, few research works have been conducted on evaluating performance of antenna/RF component under harsh space conditions, therefore its challenging to decide which type of antenna/RF components are suitable to the manufacture with which type of AM technique. Therefore, in this review, we will be considering both onboard and ground terminal SATCOM state-of-the-art implementation of AM antenna/RF component designs from the year 2019 to 2024. During this period, AM evolves rapidly towards cutting-edge AM solutions of rapid manufacture lightweight and low-cost high frequency SATCOM component prototypes.

A. AM ANTENNAS FOR SATCOM

The most suitable AM antenna types available in literature particularly for SATCOM are reviewed in this section including horn antennas, lens antennas, reflect-arrays, along with other types of antenna arrays such as phased arrays, waveguide arrays and dipole arrays. Table 2, 3, 4, and 5 provided the summary of recent state-of-the art in AM antennas, providing the manufacturing process, material used, operating frequency band, realized maximum gain and publication year.

1) HORN ANTENNAS

Horn antennas are widely considered for SATCOM, both in ground terminal and onboard satellite because of their inherent benefits such as they are simple, highly directive antennas, and less effected by structural and reproduction error as compared to patch antennas at high frequencies, where small variation can largely affect the antenna performance. They can either be used as feeding element for parabolic dish or as a standalone antenna array system. The utilization of AM technology in manufacturing of horn antennas further improves these advantages by printing cost-efficient lightweight geometries, reducing the entire weight and cost of payload for SATCOM. AM also provide excellent design flexibility which enables the fabrication of complex horn antenna structures and integrated elements that would be difficult to achieve using conventional manufacturing.

A single element, corrugate horn antenna design using AM for SATCOM is largely explored because of its complex inner structure, consists of grooves to enhance the impedance matching and radiation pattern performance providing low SLL and wide bandwidth. In [29], Ku-band corrugate horn antenna is successfully printed on lightweight PLA polymer using low-cost FDM technology, highlighting the technology's benefits over more costly, conventional CNC machining techniques shown in Fig. 4(a). The proposed antenna after metallization operates well across broad frequency range of Ku-band, i.e., 10.5-18.5 GHz with return loss value better than -20dB showing outstanding

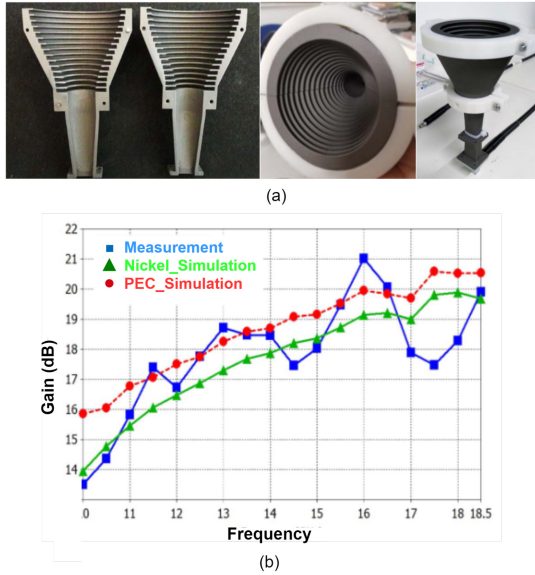


FIGURE 4. Corrugated horn antenna. (a) Fabricated prototype, (b) Gain [29].

impedance matching and low SLL of -18dB along with 14.3 dBi minimum gain as shown in Fig. 4(b). Due to fabrication method the antenna prototype has a total weight of only 232g .

The LPBF technologies including SLM and DSM are widely used to produce direct metal structures in one run, eliminating post-metallization requirements. These techniques provide good mechanical strength and electrical conductivity of RF devices as compared to other AM techniques. The author in [30] produced full metal printed axial corrugate horn antenna using DMLS technology, resulting in improved mechanical strength and electrical conductivity, eliminating post-metallization requirement shown in Fig. 5(a). The antenna simulation was done while incorporating expected surface roughness tolerances after manufacturing which ensured fabricated antenna performance within acceptable range. The linear dual polarized horn antenna successfully achieved gain of about 13.5dBi over ka-band with cross polarization better than 29dB shown in Fig. 5(b).

Another popular configuration of horn antenna for SATCOM is double or quad ridged horn. They exhibit dual-linear or circular polarization (CP) and excellent wideband performance with less complex structure as compared to corrugated horns. Incorporating single or multiple ridges in horn, the structure is successfully fabricated using LPBF AM technology [31], [32], [33]. In [31] author designed double ridged Ku-band horn antenna, which includes cone feed truncated structure, cavity with curved shaped and a mode suppressor. The SATCOM broadband properties were obtained by using the curve-shaped cavity and symmetrical radiation patterns were derived by using the truncated structure. After that, steady boresight gain was attained by using the mode suppressor as illustrated in Fig. 6(a). The antenna was manufactured in two-parts using cos-efficient

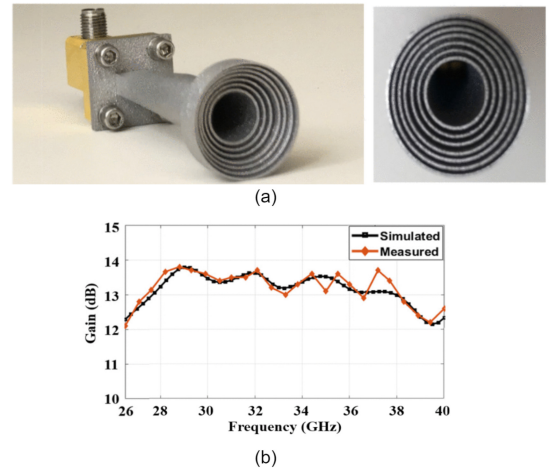


FIGURE 5. Axial corrugated horn antenna. (a) Fabricated prototype, (b) Gain [30].

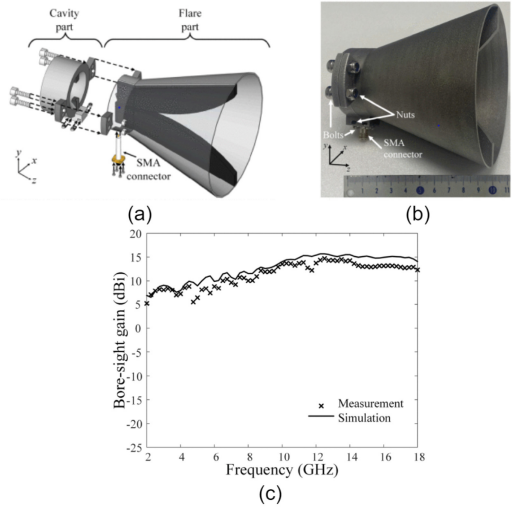


FIGURE 6. Double ridged horn antenna. (a) Structural geometry, (b) Fabricated prototype, and (c) its gain [31].

DMLS technology with aluminum alloy powder and later assembled using screws, a prototype is shown in Fig. 6(b). The achieved gain was approximately around 15dBi ; see Fig. 6(c). The results confirmed that proposed horn antenna is suitable as feeding antenna for reflectors in SATCOM. DMLS offers greater material versatility than SLM; for example, it can guarantee design performance by utilizing various metal composites.

For onboard SATCOM, it is important to design lightweight antennas yet sufficiently dense to retain electromagnetic properties. The mesh structures are well explored to achieve lightweight antenna design while maintaining antenna performance. However, careful consideration and optimization is crucial while designing and producing mesh structure. The author in [34] used SLM technique to design metallic horn antenna with reconfigurable CP for SATCOM terminal. They produce both solid and mesh structures using metal printing which gives mechanical stability to design that is one of the strict requirements for SATCOM

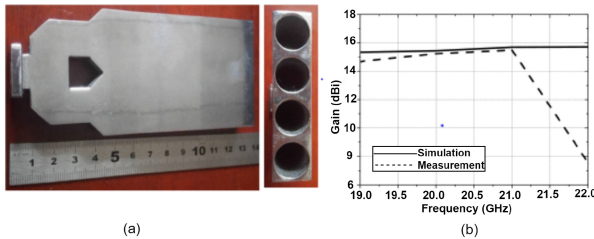


FIGURE 7. Integrated passive front end. (a) Fabricated prototype, and (b) its gain [35].

application. The reconfiguration between RHCP and LHCP was employed by combining both port beams with a phase shift of 90° . The solid structure horn antenna exhibited gain of 9.5dBi over 90% of K-band and cover part of Ka band. Further, 1mm and 1.5mm mesh structures of proposed horn antenna were also analyzed using SLM to reduce weight while maintaining the performance and stability. It was observed that due to low metal density in the 1.5 mm mesh led to poor radiation and pattern distortion. While 1mm mesh results in better performance. However, granular surface finish of SLM technology effects the antenna size therefore slightly shift in operating frequency towards the Ku-band was observed. To overcome this effect, post-printing steps are required.

Taking the advantage of AM technologies, lightweight horn antenna arrays along with complex feeding network can also be monolithically design and produced, without compromising gain and efficiency, thus providing characteristics like multibeam, high gain, wide beam scanning and high aperture efficiency at reduced cost. In [35], the author proposed a fully integrated AM passive front-end for SATCOM. The front-end design composed of a one-by-four power divider (PD), tapered waveguide, and linear array of four-element horn antennas shown in Fig. 7(a); these complex designed components are challenged to manufacture by traditional technology due to high cost and weight; therefore, SLM AM technology was used to fabricate the design. The array antenna performance well over the bandwidth of 19–21GHz with a gain of 15.1dBi and SLL better than -20dB , illustrated in Fig. 7(b). The prototype experiences the surface roughness of $1.61\mu\text{m}$ on unpolished antenna aperture which results in impedance bandwidth deterioration of 2dB and ripples in the radiation pattern of co-polarized waves, which significantly affects the performance of the front end above 21GHz. Another approach to overcome such small effect caused by surface roughness is to consider its approximation during simulation as in [33]. The monolithically integrated novel way of feeding horn antenna aperture using four-way small waveguide model was successfully printed. The complex feeding network permits optimal excitation of the aperture. The manufacturing of prototype was also done by using SLM technology. The measured result shows nearly 90% of maximum aperture efficiency which is closely related to theoretical one over 18% bandwidth for GEO SATCOM.

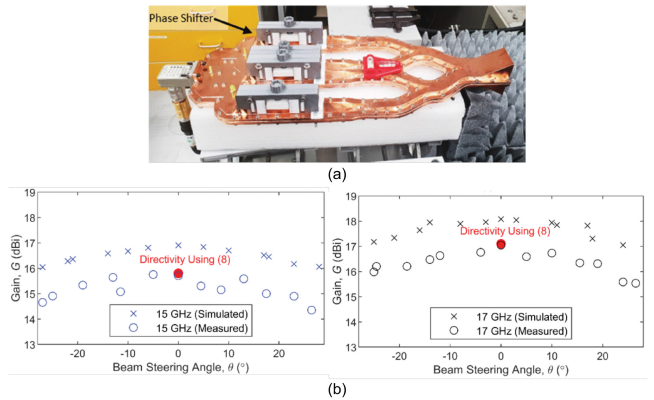


FIGURE 8. Steerable PAA subsystem. (a) Fabricated prototype, (b) its gain and beam steering angle at 15 and 17 GHz [23].

However, cost-efficient approach to acquire high-resolution manufacturing of complex intricate beam-forming network can be done by using two different AM technologies together like Shin et al. in [23], designed four-element steerable Ku-band PAA subsystems together with a beam-forming network of seven metal-pipe rectangular waveguide (MPRWG) components and fabricated it using Polyjet and low-cost FDM technique together.

The main body of complex structure is manufactured using high-resolution polymer based Polyjet AM, while the FDM technique was used to fabricate dielectric slabs using premium ABS filament for tunable phase shifters and PLA filament was used in the manufacturing of calibrated screws and mounting brackets, later sand polish was done on FDM parts to improve surface finish. The main body of PAA, after fabricating using Polyjet, undergoes a metallization process using metal electroplating as shown in Fig. 8(a). Overall, a 1-1.5dBi variation between measured and simulated gain was observed, but there was an excellent agreement between measured and predicted results of beam steering angles see Fig. 8(b). The discrepancy in gain is due to finite metallization conductivity, surface roughness, and other minor impacts of AM on prototype design such as use of polymers as a base material. By combining these two printing techniques, it was possible to print complex antenna design at a significantly lower cost and 86% weight reduction compared to typical manufacturing methods. Further weight reduction is also possible by replacing waveguides with flanges to join individual components.

The FDM and SLA provide a good trade-off between the accuracy and manufacturing cost, but they require two-step process which may suffer from non-homogenous metallization because it is challenging to control the material deposition. Moreover, after metallizing, the split-block configuration needs to be precisely assembled using screws and proper alignment is crucial for optimal performance which is also challenging. Therefore, author in [36] designed monolithically integrated horn antenna array incorporating 90° twisted waveguide structure as shown in Fig. 9(a).

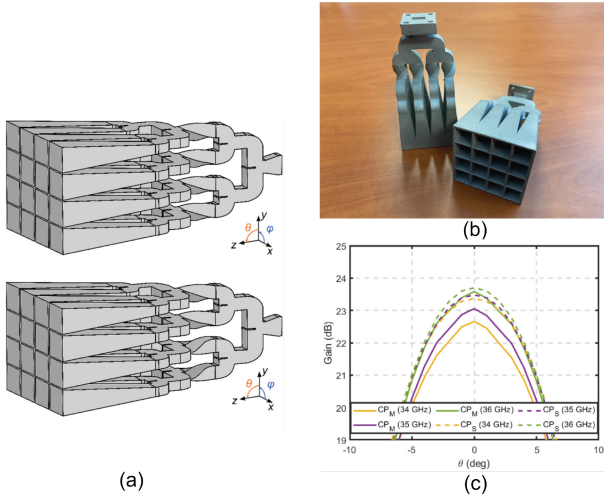


FIGURE 9. Metal-only Horn antenna array. (a) Antenna geometry with twisted feeding network, (b) fabricated prototype, and (c) its gain [36].

This novel approach enables simplified feeding network in which same H-plane power divider is utilized in both vertical and horizontal networks. The horn antenna array with complex geometry of the feeding network was successfully manufactured using LPBF technology with 316L steel material as shown in Fig. 9(b). Due to inherent rough surface finish of LPBF, postprocessing was done using sandblasting on the outer surface of the antenna. After fabrication, the antenna prototype exhibited elevated temperature due to which structure might suffer thermal deformations. To minimize the risk, author suggested thermal optimization of the antenna by incorporating multiple thickness values, thereby enhancing its structure stability after fabrication. The antenna has 2.5GHz of bandwidth at the central frequency of 34.7GHz with maximum gain of about 26.6dB at 36GHz and total radiation efficiency of 80% in 34-36 GHz band shown in Fig. 9(c).

Researchers use AM techniques to manufacture different horn antenna structures according to their application and each claim to be used for SATCOM. The choice of AM technique to design horn antennas with complex inner structure such as corrugate horns [29], [47], axial corrugated horn [30], single or double ridge horn [31], [32] is critical because precise fabrication of grooves and ridges is essential. SLA AM technology is preferable for such intricate geometries and provide high resolution with excellent surface finish. Recently SLA has been largely explored for space application due to use of polymer resins which results in lightweight structures [49]. However, resultant prototypes are brittle and may encounter challenges in space environment. On the other hand, metal based LPBF technologies are also widely considered in literature for SATCOM, as reported in [36], [50]. But these technologies suffered from low surface finish and dimensional accuracy which can be encountered by carefully incorporating surface roughness

parameters during simulation as in [33]. The prior consideration of SLM limitation successfully allows fabrication of intricate geometry. Likewise, DSLM technique is also an excellent option to print highly integrated lightweight structures in cost-efficient way. To improve the surface quality, further post-processing techniques can be applied including polishing, coating, or chemical etching. Table 2 shows the characteristics of different types of AM horn antennas for SATCOM.

2) LENS ANTENNAS

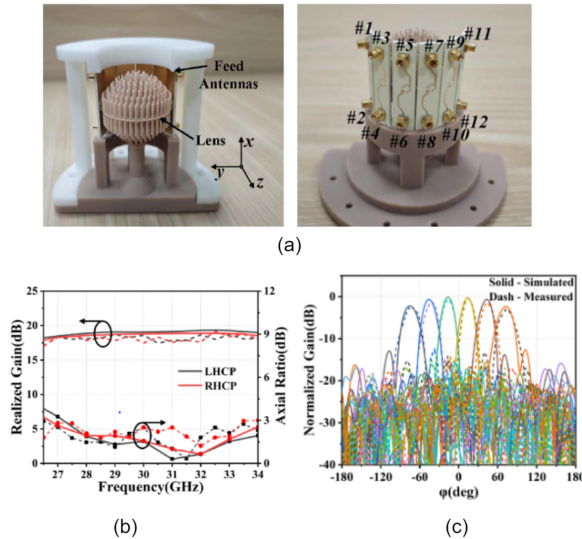
After the advancements in AM technologies in RF domain, the lens antennas have also become the powerful candidate for SATCOM. They exhibit dielectric structure with feed antenna. Lens antennas work on the principle of wave (emitted from source antenna) manipulation through refraction which can be done by varying lens material properties. These lens antennas are of two types: homogeneous and nonhomogeneous lens. The radiation properties of homogeneous depends on the shape of lens and for nonhomogeneous lens, also called Gradient Reflective Index (GRIN) lens, associated not only by shape and size but also with reflective index distribution along lens profile [51], [52], [53]. Previously implementation of such complex lens antenna structure configuration becomes difficult and costly to realize by using traditional manufacturing due to limited control over shape and distributive material properties [54]. Flexibility of customizing shape and material properties in AM has made lens antennas available for SATCOM, which opens the door for compact, high gain and cost-efficient antenna solutions providing benefits like wide beam scanning, beam shaping, wideband performance, and dual polarization [22], [55]. Hence minimizing system complexity and cost associated with feeding networks of traditional phased arrays and parabolic dish antennas for SATCOM [56], [57], [58].

GRIN lens is the popular configuration of lens antennas, which rapidly evolve after the advancements in AM technology. In paper [52] the author gives detailed overview of GRIN lens antennas realized using AM technology. These types of lens antennas exhibit highly directional properties, low SLL and wide scanning angle which are the basic requirements for SATCOM. To design GRIN lens, polymer-based AM techniques are mostly employed such as FDM and SLA, however few works have also utilized metal-based AM techniques SLM and DSLM to realize GRIN lenses but not for SATCOM. Therefore, future work is required to produce GRIN lens antennas using metal-based AM techniques for SATCOM as they provide high mechanical strength, durability, and electrical conductivity.

The Luneburg lens (LL) antenna is among the most commonly used types of GRIN lens antenna due to its capability to achieve multibeam radiation pattern, wide beam steering with minimum scan in cost-efficient way [60]. By positioning array consists of magnetoelectric (ME) dipole fed via SIW as source along the LL surface printed with low-cost SLA; LP beam with scanning angle of $\pm 60^\circ$ was

TABLE 2. AM horn antennas for Ku, K and Ka-band SATCOM.

Ref	Antenna Type	Technique	Material	Band	Gain (dBi)	Year
[23]	Waveguide fed horn antenna array	DMLS	AlSi10Mg	Ka	27.5-33.8	2019
[29]	Conical Corrugated horn antenna	FDM	PLA,Nickel	Ku	14.5	2019
[38]	Steerable Phased Array antenna	FDM, Polyjet	ABS, VeroWhite Resin	Ku	14.4	2019
[38]	Horn antenna	DMLS	AlSi9	Ka	14.31	2019
[30]	Axial Corrugate Horn	DMLS	AlSi10Mg	Ka	13.2	2020
[39]	GRIN dielectric double-ridged horn	SLS	Nylon PA2200	Ku	10	2020
[30]	Axial Corrugated horn	DMLS	AlSi10Mg	Ka	12.4	2020
[40]	Mm-wave horn antenna	DMLS	AlSi10Mg	Ka	6.1-11.4	2020
[41]	4x4 double-ridged waveguide antenna array	DMLS	AlSi10Mg	Ku	16	2020
[33]	Quad-Furcated horn	SLM	AlSi10Mg	Ku	18.4	2021
[42]	Lattice structure antenna array	SLM	AlSi10Mg	Ka	Not-defined	2021
[43]	Dielectric Rod antenna	FDM	ABS,PLA, PeTG	Ku	13.1	2021
[44]	Horn Antenna integrated OMT	DMLS	AlSi10Mg	Ku	Not-defined	2021
[32]	Quad-Ridge horn antenna	SLM	AlSi10Mg	Ka	12-15	2022
[45]	Dual-band DP Horn Antenna Array	DMLS	AlSi10Mg	Ku	26.48-26.51	2022
[46]	4x1 Horn antenna array	LPBF	AlSi10Mg	Ka-band	No-defined	2022
[31]	Double-ridged horn antenna	DMLS	AlSi10Mg	Ku	20.7	2023
[47]	CP Horn Antenna array	SLM	AlSi10Mg	Ka	Not-defined	2023
[48]	Choke Corrugated Gaussian Profile horn antenna	FDM	Electrifi Conductive Filament	Ka	20	2023
[49]	Duplexer horn antenna array	SLM	AlSi10Mg	K/Ka	26.1-31	2024

**FIGURE 10.** LL fed via ME dipole array. (a) Fabricated prototype, (b) it's gain, and (c) beam scanning angle [59].

achieved in [61]. Applications such as low-orbit SATCOM can benefit from the advantages of dual CP design, in anti-interference and anti-multipath fading. Therefore, author in [59] designed dual CP spherical LL antenna which was fed via dual-LP six element ME dipole array antenna as shown in Fig. 10(a). The LL was designed in such a way which converts dual LP waves of feed antenna into dual CP waves. The SLA AM technology was used to enable flexible distribution of effective permittivity of resin with ϵ_r

= 3 across the lens profile to realize transforming dual LP into dual CP wave. The unit cell was produced by adjusting the size of dielectric column and combined it with air. The complex lens structure consists of 21 layers; 7 layers in horizontal and 14 layers in vertical direction. Novel design of LL increases gain from 17.8 to 19.2dBi as compared to separate fed ME array, and an axial ratio (AR) less than 3dB with BW efficiency of 23.3% as shown in Fig. 10(b). Due to multiple feeds, approximately $\pm 81^\circ$ scanning across wide angular range is achieved see Fig. 10(c). The feeding structure was fabricated using traditional PCB technology.

Other popular layout of LL is parallel plate waveguide (PPW) LL, introduced to minimize the size of AM spherical LL whose diameter is 4λ which is practically large and too heavy for SATCOM [62]. In [63], a PPW LL was produced using SLA based AM which successfully achieved wideband CP waves using LP horn as a feeding element. The author used FLGPCL02 polymer resin to fabricate LL and to avoid breakage, wall thickness of dielectrics was set to be 0.8mm. FDM AM technique was used to produce horn and holding fixtures, suggested pre-heating platform upto 50°C and printing tip for PLA was set at 210°C to avoid limitations of FDM technique. Further metallization process was carried out using adhered copper foil which also reduces the surface roughness of SLA and FDM printed structures as shown in Fig. 11. However, incorporating two techniques a manufacturing of low-cost antenna system operating in Ka-band was successful achieved.

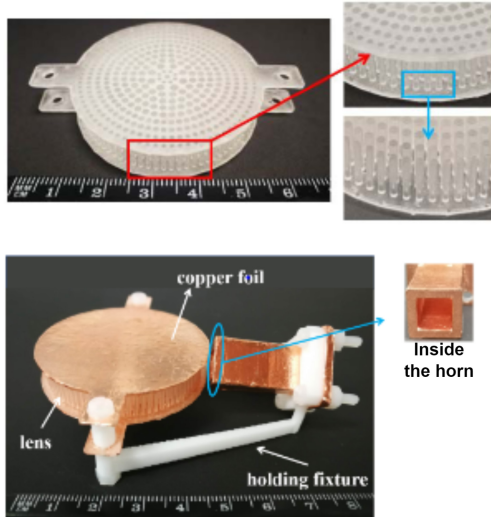


FIGURE 11. PPW LL fed via horn antenna [63].

Incorporating two techniques may result in misalignment and low conductivity which degrade the performance, therefore author in [64] designed compact and lightweight, multibeam metal-based half Luneburg geodesic lens antenna as single-piece structure. This design overcome the challenge of misalignment problem using multiple layers which results in high SLL caused in traditional manufacturing technique. The author replicate [65] and successfully achieved single-block lens antenna using LPBF as shown in Fig. 12(a). The fabrication quality and structural integrity depends on orientation of the manufacturing process; therefore, the author adapted suitable inclination of 45° that ensures the resistance and rigidity of feed zone during AM. Fig. 12(b) shows that prototype achieved similar performance characteristics by using LPBF AM technology while significantly reducing material usage and processing time, enabling cost-efficient and high-performance lens antenna design.

Despite the easy fabrication and satisfying performance of AM LLs, still there are problems associated with sensitive polarization, fragile structure and non-disposed support, which weakened the structure and effects the performance after been deployed for SATCOM. Therefore author in [66] proposed quasi-icosahedron (QICO) models which helps to discretized the structure of LL in such a way that proposed geometry solve the above mentioned problems effectively. In the paper unit cell has triangular geometry rather than normal ring type structure and oriented towards the center which helps to maintain stable radiation pattern and CP transmitting waves, that are sensitive to incoming wave polarization. Such advantage of icosahedron LL saves the trouble for feeding alignments. The lens was printed using SLA technique with FormLabs printer and FLGPCLO2 polymer resin was an inclusion material. The prototype exhibits 48mm diameter and 2.4 mm thickness of each layer which make it print compatible. Polymer based LL structure make the lens mechanically unstable, but QICO geometry enhance the

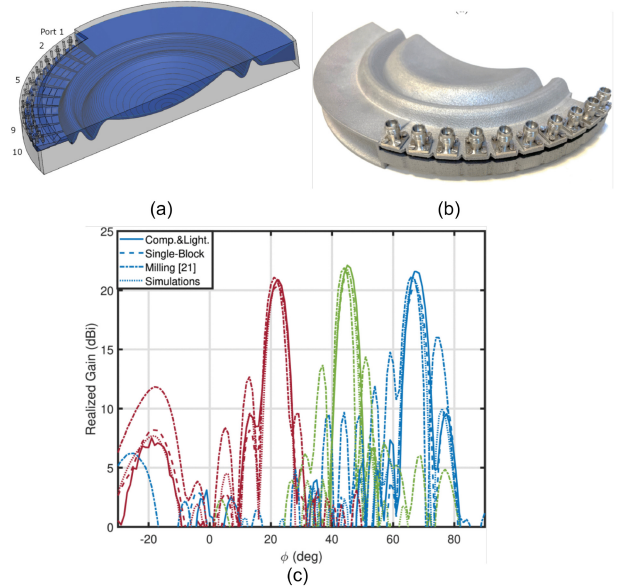


FIGURE 12. Compact & lightweight multibeam Luneburg geodesic lens antenna.
(a) Simulated geometry, (b) fabricated prototype, and (c) its comparison gain results [64].

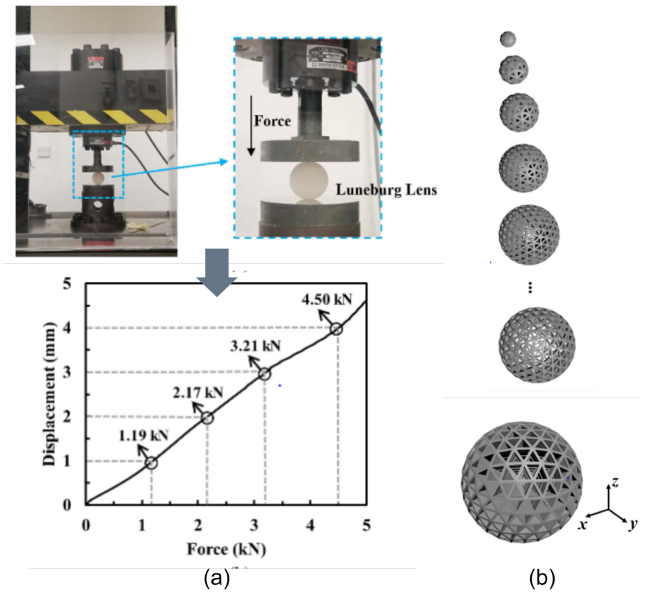


FIGURE 13. QICO model LL, (a) Durability testing and (b) QICO LL geometry [66].

durability of AM prototype as shown in Fig. 13(a), only 8% displacement was caused when 4.50 kilonewton (kN) force is applied and according to earth's gravity $g=9.8\text{N/Kg}$, maximum weight of 459.18kg can be handled by such lens structures. As illustrated in Fig. 13(b), different triangles that make up the LL support each other. All of these benefits of QICO model make LL geometry compatible with AM technology.

By definition, a spherical lens necessitates that the feed antenna should be positioned at specific distance away from the lens surface. Particularly in systems that need several

feed antennas for beam steering, this might result in intricate mechanical design and alignment problems. Hence modified LL geometry was analyzed in [67] using quasi-conformal transformation optics (QCTO) which allows to transform spherical LL into flat shaped LL without degrading its EM properties. The calculated distribution of permittivity using QCTO, was physically implemented using low-cost FDM technique. The prototype was easily manufactured, having 24dBi gain over Ka-band and successfully achieved beam steering of $\pm 90^\circ$ with 1° increment. However, convenient fabrication of flat LL having reduced volume and fits into any communication system can also be achieved by implementing planar structure possess varied refractive index across the plan such that the design utilizes different dielectric layers in ring structure [54], [68]. Previously such structures were difficult to fabricate using traditional milling methods, but now these complex design geometries are manufactured easily using AM technology and associated variety of materials available. In article [69] author designed ring layers with different relative permittivity that transforms spherical wavefront into planar wavefronts. The structure is easily implemented by utilizing ABS filaments of different permittivity for each layer and altering infill percentage of available ABS filaments other levels of layers are achieved, as illustrated in Fig. 14(a). The substantial permittivity variation at the air-lens transition, particularly for the middle rings, which can result in notable reflections, therefore matching layers consists of two filaments have been designed and combined with lens to mitigate the effect. The SLA AM printing technology is used to fabricate each ring individually and then glue is used to combine the whole structure along with matching layer shown in Fig. 14(b). The lens achieved wide beam scanning over Ka-band with 10dB of maximum antenna gain.

Apart from polymers, LL antennas have also been composed of ceramic materials and ceramic-based SLA (CSLA) is commonly used to fabricate the dielectric ceramic LL antennas with high accuracy. The author explored various ceramic materials and successfully prepared LL using AM technology [70], [71]. They are preferred because of their high dielectric constant, thermal stability, and low dielectric losses. Ceramics can withstand high power and exhibits exceptional temperature and corrosion resistance as compared to polymers, making them appropriate for long-term durability and performance in harsh space environment.

For example, in [72] printing and sintering process of LL is discussed using MgTiO₃-CaTiO₃ ceramic with SLA technology. It was analyzed that adding more CaTiO₃, which has a strong UV absorptivity, the ceramic slurry's curing depth drops. Furthermore, a layer dislocation error happens during molding when the cure depth is smaller than 0.1 mm. Therefore, one of the key criteria for determining whether or not a material may be used in stereolithography is its UV absorptivity. The material possesses high dielectric constant of 17.8. The flat LL prototype achieved high radiation efficiency along with 19.1 dBi gain over entire Ku-band.

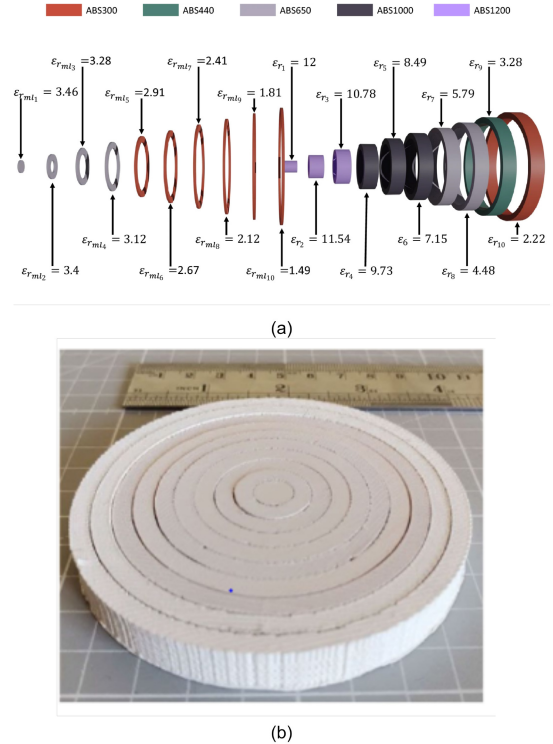


FIGURE 14. Multiple ring layer LL, (a) Layer configuration and (b) Fabricated prototype [69].

In conclusion, ceramic slurry is required to fabricate LL antennas with desired performance parameters. The viscosity of the ceramic slurry is meticulously regulated to guarantee even spreading during printing and to avoid the structure collapsing during production. The slurry must exhibit shear thinning behavior allowing for properly shaped structure. Furthermore, the ceramic slurry is created with a certain curing depth to determine the extent to which UV light penetrates and hardens the single layer of slurry. This element is essential for guaranteeing both layer adhesion and the precision of the AM printed object. The UV absorptivity of the material is also the important parameter that affects the curing depth. Traditional production techniques would be unable to achieve the requisite electromagnetic properties of the antenna and successful printing due to the particular composition of the slurry. Thus, by combining the advantages of high-performance ceramic materials with the adaptability of AM printing, intricate geometries with accurate dielectric constant control are easily obtained.

Another advanced variant of LL is Gutman Lens (GL), poses an internal focal point for fed. The size of GL is smaller than LL, which benefits the GL in size-constrained applications. However, such type of structure experience fabrication challenges as fed source is placed inside the lens. One way to solve, is by truncating the lens across its center, providing a surface for mounting source antenna [73]. In [74], the fully dielectric AM GL is designed using FDM technology. Fabricated GL operate at Ku-band with realized

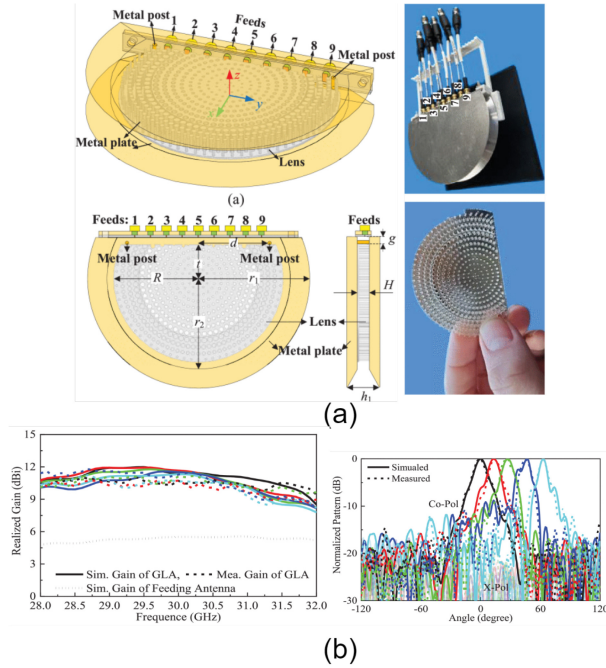


FIGURE 15. Truncated 2D GL antenna, (a) Geometry with fabricated prototype, (b) its gain and co-pol [75].

gain of 20 dBi and broadside beam steering of $\pm 45^\circ$ with 3dB scan loss. Another truncated Gutman Lens is designed using SLA AM printing technology with FLGPCLO2 resin material having permittivity of 2.9 and a loss tangent value 0.02. An mm-wave truncated 2D GL antenna with planar-fed structure and wide beam scanning was investigated. It can be seen in Fig. 15(a) that traditional design of PPW is also added to the top and bottom plane of the GL to enhance its impedance matching and radiation performance. To improve the beam scanning while keeping its original permittivity distribution, two metal supports near the feeds edge were introduced. Moreover, the dielectric material and corresponding air-hole cells composed of same material were combined to create varying gradient index permittivity needed to design the GL which prevent the usage of multi-material and facilitates AM printing process. Author analyzed that the losses associated with AM material, the highest achievable gain is 11.3dBi and if these losses are eliminated maximum gain of 14.7 dBi was obtained at 45° , and deviation in gain over wide-beam scanning was minimum around 0.7dB with cross-polarization range lower than -20dB shown in Fig.15(b) [75].

The other types of lenses for SATCOM provided in literature such as Fresnel lens [76], [77], [78], [79], Eaton lens [80], [81], and Mikaelian lens [82], [83], [84] have also now been developed using AM printing technology. Out of them, Fresnel lens has recently been investigated for SATCOM in [85]. The author uses FDM technique and PLA as base material to manufacture the lens prototype. The FDM printer (Ultimaker2+ extended) has nozzle size of 0.4mm which produce minimum layer thickness of 0.02mm and

approximately 3.6mm of step height. However, the fabricated lens experience surface roughness of 0.4mm which limit the performance of lens at 30GHz which can be improve by using techniques having high resolution and surface finish.

Apart from GRIN, AM metamaterial lens antennas have also been analyzed for SATCOM [96]. Kim et al. [92] AM deployable metasurface lens antenna using inkjet printing for onboard SATCOM. The unit cell structure consists of three metal layers separated by two PLA dielectric layers and one Kapton layer. Top and bottom metal layers contain two orthogonal grating for x and y polarization while Kapton consists of I-shaped pattern which effect amplitude and phase of EM wave. However, folding and unfolding operation of the structure is carried out using origami structure which AM using thermoplastic polyurethane (TPU) filament and PLA. Flexibility and durability of TPU is higher than PLA therefore upper and bottom layer holding the metalens and source antenna were AM using PLA and middle layer was AM printed using TPU to provide efficient deploy ability. The proposed meta lens provides wide beam scanning of around 360° and 10dB impedance BW over frequency range of 24.0-34.9 GHz. The I-shaped pattern printed using inkjet printing, incorporating tolerance level 14 μm for widths and 25 μm for gaps. The manufacturing tolerance and structure assembly after fabrication slightly effects the gain and efficiency of meta-lens antenna but the overall metalens performance well. Hence lightweight, cost-effective and compact onboard lens antenna design is successfully achieved using two AM techniques. Additional designs of lenses for SATCOM such as hyperbolic [86], [88], [93] and ellipsoid [91], [95] are also investigated either using low-cost FDM or high accuracy SLA AM technology.

In conclusion, to produce lens antennas the FDM technology using PLA polymer is better for cheap and fast fabrication with compromising accuracy, and it require support structure for overhanging parts, which can be avoided by either printing lens in two halves or using tapered transition [90]. It is user friendly process and can print both non-conductive (polymers) and conductive (filaments) materials but with relatively low conductivity while non-conductive require post-metallization which is preferable over filaments. The lens antenna structures mostly required varied permittivity which results in intricate geometry that are sensitive to variation in dimension, therefore careful consideration is required while using FDM technique. The FDM print using filaments on a continuous spiral design and tuning on/off, the structure would provide highly accurate control of infill dielectric constant versus radius [87], [92]. Moreover, for highly accurate and high-resolution design, SLA and SLM technologies can be used [86]. But these technologies are expensive and require skilled users to operate. On the other hand, jet printing technology can also provide high resolution and can be used for fabrication but only drawback is the high cost of conductive inks [92]. However, hybrid techniques are also widely adopted in

**TABLE 3.** AM lens antennas for Ku, K and Ka-band SATCOM.

Ref	Antenna Type	Technique	Material	Band	Gain (dBi)	Year
[22]	Integrated Lens	FDM	PLA	Ka	15.6	2019
[62]	Luneburg Lens antenna	SLA	Photopolymer VeroClear	Ka	21.2	2019
[87]	2D beam scanning Lens antenna	SLA	Resin	K	23	2019
[61]	3D Luneburg Lens antenna	FDM	PLA	Ku	14.7	2019
[88]	Fresnel Plate Lens antenna	SLA,FDM	Resin, Premix	K	27-33	2019
[67]	Dual CP Luneburg Lens antenna	SLA	Photopolymer resin	Ka	19-21	2020
[73]	Flat Luneburg Lens antenna	SLA	Ceramic MgTiO ₃ -CaTiO ₃	Ku	18	2020
[64]	Parallel-plate CP Luneburg Lens antenna	SLA	Photopolymer resin	Ka	20	2020
[88]	Hyperbolic flat lens	FDM	Premix ABS	Ka	20	2020
[89]	Corrugated Plate antenna	Polyjet	VeroClear material	Ka	18.5	2020
[63]	2D PPW Luneburg Lens antenna	SLA	Resin	Ku	14.7-15	2021
[72]	Luneburg Lens	SLA	Ceramic Al ₂ O ₃	Ku	15	2021
[86]	Fresnel Zone Hybrid Lens	FDM	ABS, PREPERM	Ka	13.3-25.6	2021
[91]	Material-optimized Lens antenna	FDM	PLA	Ku/K	23.7	2022
[92]	3D printed lens antenna	SLA	Resin	Ka	15.8	2022
[93]	Metasurface Lens	Inkjet	PLA, Kapton	K	18.3	2023
[94]	Mirror folded lens	SLA	Nylon	Ku	26.5	2023
[55]	GRIN CP stepped Lens	SLA	Not-defined	Ka	24.8	2023
[95]	Half-Gutman lens antenna	FDM	Thermoplastic	Ka	25.3	2023
[60]	Dual CP multibeam Luneburg Lens	SLA	Photosensitive Resin	Ka	19.2	2024
[96]	Wide CP ILA	SLA	Nylon	Ka	23.1	2024
[97]	Conformal Meta-Lens	FDM	PLA	Ka	15.1	2024

manufacturing of cost-efficient and high-performance lens antenna structures for SATCOM as in [87].

The study highlights the need to account for substrate losses during the design of these types of lens antennas, as they significantly impact performance. The authors note that improved radiation efficiency could be achieved by using a material with a lower loss tangent, although that may come at a higher cost [55]. However, customized materials can be used and it is suggested to firstly investigate the epsilon and loss tangent of customized dielectric involve in configuration of lenses, higher dielectric constant employed with large void gaps enhances the efficiency and availability of various material choices. Summarized different characteristics of AM lens antennas for SATCOM are listed in Table 3.

3) REFLECTARRAY ANTENNAS

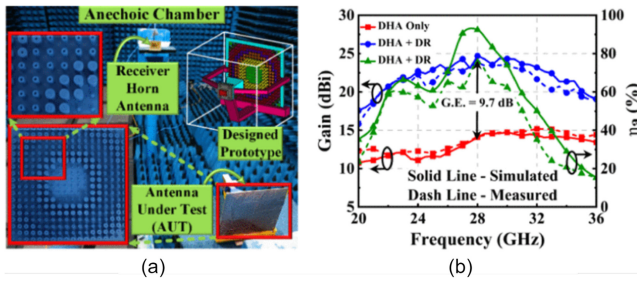
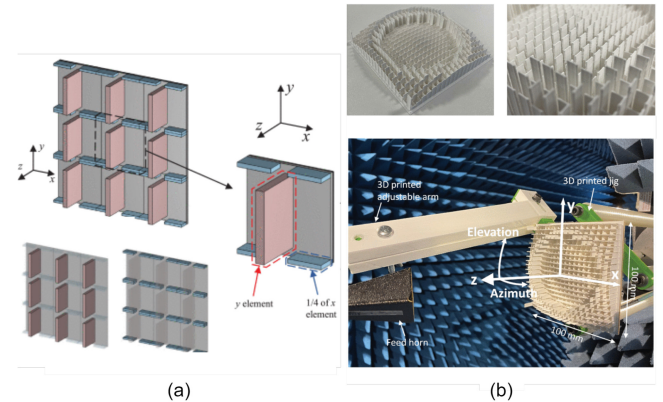
High gain antennas are very important for long-distance SATCOM. The most common practice to increase gain and efficiency is the deployment of parabolic reflector and phased array antennas (PAAs). The precise configuration of parabolic reflectors and large complex feeding network requirement of PAAs, occupy space and increase weight, which are very crucial for onboard SATCOM. Many types

of alternatives for antenna subsystem have emerged in which reflectarray antennas are strongly considered. They are made of array elements having different phase distribution that allows incoming wave from feed source to radiate in desired direction that's why they do not require bulky feeding networks and successfully provide high gain over 30dbi [97]. At high frequency fabrication of reflectarrays required low-loss laminate substrates which are very expensive. Therefore, with the advent of AM technology, manufacturing of low-cost and lightweight reflectarrays (RA) at high frequency have also been possible without compromising on performance parameters in single print. Table 4 shows that RA mostly prefer dielectric structure fabricated using SLA or FDM techniques with dielectric material mainly composite filaments. However, few research has also focus on metal-based RA structures print using AlSi10Mg enlisted in Table 4.

Recently, [109] author proposed AM all-dielectric reflectarray (DR) fabricated using low-cost FDM technique with 100% infill ratio of Acrylonitrile Butadiene Styrene ABS400 PREPERM material filament which is best suited for onboard SATCOM as compared to other filaments because it provides high resistance to extreme thermal cycle in space atmosphere.

TABLE 4. AM reflectarray antennas for Ku, K and Ka-band SATCOM.

Ref	Antenna Type	Technique	Material	Band	Gain (dBi)	Year
[99]	OAM Reflectarray antenna	FDM	Preperm ABS10.0	Ka	20	2020
[100]	Polarization Reconfigurable Reflectarray antenna	ND	AlSi10Mg	Ka	25.3(LP) 26.0(RHCP) 25.8(LHCP)	2020
[101]	CP Dielectric reflectarray	FDM	filament	Ka	24.2	2020
[102]	Dielectric Resonator reflectarray	FDM	ABS PREPERM	30-40 GHz	22.53	2021
[103]	Dielectric broadband reflectarray	FDM	PLA,PREPERM, ABS	K	23.3	2021
[104]	Deployable Dielectric reflectarray antenna	SLA	Flexible 80A resin	mm-wave (26-34GHz)	24.6	2022
[105]	Dual CP dielectric reflectarray antenna	FDM	PREPERM	Ka	27.9	2022
[106]	Metal-only reflectarray antenna	ND	AlSi10Mg	22-25&31- 34 GHz	24.5	2022
[107]	Metal-only reflectarray antenna	SLA	High temp resin	Ka	27-30	2023
[108]	Dielectric perforated reflectarray	Polyjet	Verowhite plus, Dielectric	Ka	30.8	2023
[109]	Dielectric Reflectarray Antenna	FDM	ABS-400 PRERERM	mm-wave (20-36GHz)	20	2024

**FIGURE 16.** FDM printed DR, (a) fabricated prototype, (b) it's gain and efficiency [109].**FIGURE 17.** LP-CP dielectric RA, (a) unit cell geometry, (b) fabricated prototype [104].

The horn antenna was also produced using FDM technique as feeding element for DR. However, FDM technique have low dimensional accuracy, but keeping the bed and nozzle temperature as 100C and 240C, successful fabrication of DR has been carried out to have acceptable performance. The overall printing process took about 12h. The DR provide wide BW performance at high frequency Ka-band with peak gain of 23.8dBi and 75% aperture efficient shown in Fig. 16. It has the compact aperture size of $54 \times 54 \text{ mm}^2$ which make it suitable contender for onboard and ground terminal SATCOM. Because of the printing parameters, the prototype took a long time to construct. This was due to the fact that the low-cost FDM method requires a trade-off between printing time and resolution because it only produces sufficient precision when the object is printed slowly.

The RA with CP is important for SATCOM because linear polarized waves will suffer with high atmospheric losses. Hence [104] author designed Ka-band LP-CP dielectric-based RA which provide wideband transformation of LP-CP wave with $\pm 90^\circ$ phase shift and maximum gain found to

be 27.9dBi with 38% left and 34% right aperture efficiency. The unit cell design shown in Fig. 17(a) composed of two integrated LP components in orthogonal direction with equal magnitudes and $\pm 90^\circ$ phase difference. The design was fabricated using Raise3D Pro2 FDM printer with PREPERM TP20755 material. The printer extruder size was 0.4mm and layer height was selected as 0.01mm for optimum unit cell design. To guarantee accuracy of fabricated prototype, small portions of RA were printed initially to adjust the printing parameters and then print entire RA accordingly. The fabricated RA is shown in Fig. 17(b).

Deployable antenna structures have been extensively explored because they occupy small space, which is important for satellite. However, most of the AM RA uses rigid dielectric material which limit the deployability. The author in [103] proposed deployable dielectric RA inspired by origami art which provide high gain of 24.6 dBi with $\pm 10^\circ$

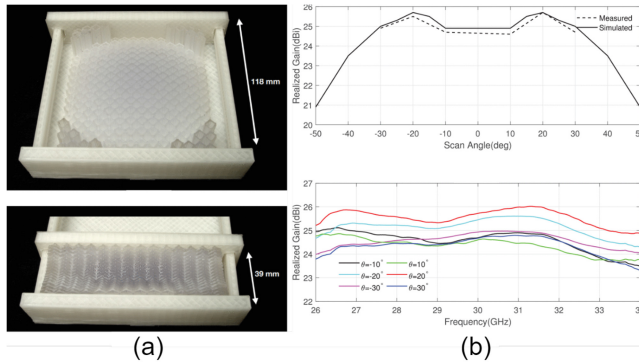


FIGURE 18. Deployable dielectric RA, (a) fabricated prototype, (b) scanning angle and its realized gain [103].

to $\pm 30^\circ$ beam scanning over K-band with aperture efficiency of 22.8% see Fig. 18(b). The proposed RA manufacture with SLA technology and uses formslab flexible 80A resin which provide flexibility to ensure deployed and retracted state in one geometry. After fabrication, the prototype undergoes post-processing steps such as alcohol wash and curing to ensure surface finish and accuracy. The prototype of dielectric RA successfully saved 65% volume in its retracted state as shown in Fig. 18(a).

After successfully realizing dielectric-based RA using AM technologies, few research has proposed efficient design prototype using FDM that withstand harsh space environment. Nevertheless, these polymer-based all-dielectric RAs may suffer from low power-handling capability which is also crucial for high-power SATCOM. Therefore, AM all-metal RA antennas are realize as suitable replacement. In [105], AM metal only RA is designed using AlSi10Mg alloy powder as it provides good conductivity. The unit cell consisted of an anisotropic metal block set on the whole metal surface was employed. Phase shifting was achieved by vertically modifying the position of unit cell and Pancharatnam-Berry (PB) geometric approach achieved high-band phase shifting by horizontal rotating the metal block. In addition, LHCP horn antenna was also designed as the feed. The design achieved peak gain that ranges from 20.2-24.3dBi over low band (22.5 to 25.5 GHz) and 22-24.5dBi over high band (31.0 to 34.5 GHz) and observed a phase shift around 0° to 180° . The small discrepancies observed in measured results were due to surface roughness of LPBF technology which can be avoided while incorporating it during simulation. The proposed design is the potential candidate for high-power onboard SATCOM.

Another option is to use SLA technology and perform post metallization, because it prints smooth surface with high dimensional accuracy. For example, authors in [106] proposed metal-based RA prototype which was fabricated with SLA technology using high temp resin and following silver metallization. Independent control for orthogonal polarization in RA is difficult to realize using metal-only, most of them uses traditional PCB stack layering technology

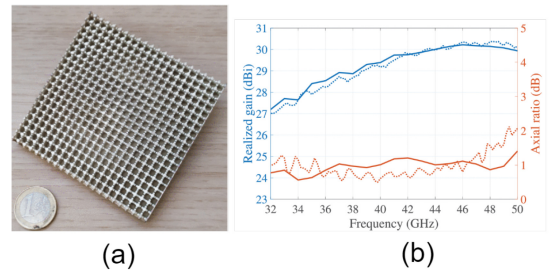


FIGURE 19. LP to CP RA, (a) fabricated prototype followed by silver metallization, (b) axial ratio and its realized gain [106].

with dielectric in between them. However, advancements in AM allow 3D unit cell design for RA which provide efficient control over orthogonal polarizations in wideband and thus allow LP to CP RA design with an AR<1.5dBi. The metallization process was carried out using silver spray by a company called jet metal technologies. The thickness of the silver coating was $2.5\mu\text{m}$, which is roughly seven times the surface depth at the lowest operating frequency. This metallization technique produces an average roughness of $2\mu\text{m}$, which degrades the conductivity achieved by silver [110]. The conductivity is still maintained at about $3\cdot10^7$ S/m, thus drop in conductivity is negligible. Using SPARK3D software, the prototype's power-handling capacity was determined to be 8699 W per unit cell. The fabricated prototype is shown in Fig. 19(a). The performance of prototype after metallization provides good agreement with simulation. The gain varies from 27 to 30.3 dBi with radiation efficiency greater than 97% over the wide range of frequencies from 32 to 50 GHz as shown in Fig. 19(b). Since the high-temperature resin material has exceptional mechanical strength, the RA is effective for SATCOM applications and appropriate for onboard SATCOM.

Low-cost FDM technology is commonly adopted to print all-dielectric RAs using different composites such as in [101] dual-polarized dielectric RA was fabricated using PREPERM ABS DK10.0 filament from premix which has high dielectric $\epsilon_r = 10$ and low loss tangent 0.003. The manufacturing process took almost 1hr 40minutes with nozzle and bed temperature set at 235°C and 105°C , specified for the required filament. The overall low profile of 0.21λ RA is observed which is due to using high permittivity material and it also realized independent dual polarization which has not been done in [98]. However, the discrepancy was observed in measured results which is due to surface roughness and printing precision. Other authors in [98], [100], [102], [107] have also used filaments which greatly reduce the size and weight of dielectric RA, but they aren't feasible for high-power SATCOM and these filaments except [109], are also not efficient for onboard SATCOM. However metal-based AM of RA in [99], [105], [111], using AlSi10Mg has been successfully realized for both onboard and ground base stations because of their efficient performance in harsh

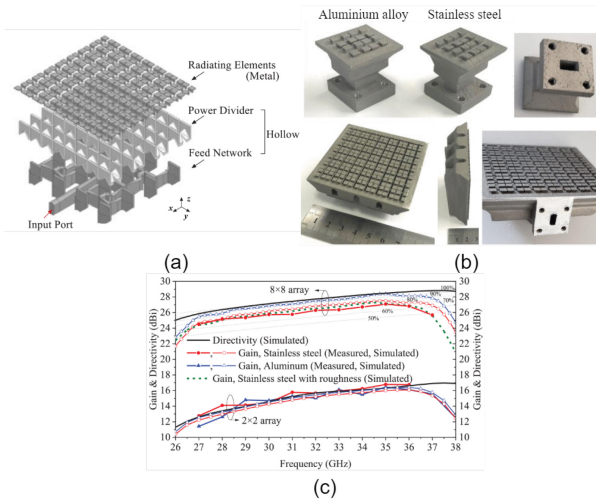


FIGURE 20. ME dipole antenna array, (a) structural geometry, (b) fabricated prototypes, (c) realized gain & directivity [118].

space environment and has good power-handling capacity in contrast to filament based FDM technique.

4) ANTENNA ARRAYS

In addition to above mentioned RAs and horn antenna arrays, AM antenna arrays using dipoles [112], [113], waveguides [41], [114], [115], [116] and patches [42], [117] are also widely used for SATCOM because they increase effective spectrum ranges, build long distance communication while maintaining size requirement. AM antennas arrays for SATCOM are summarized in Table 5.

In [118] author designed dual polarized 8x8 ME dipole antenna array with air-filled waveguide feeding network. It consists of 2x2 ME dipole antenna subarrays. The unit cell has two layers; top layer consists of ME-dipoles with metallic self-supporting structure fed via cross-shaped waveguide, and bottom layer consists of feed cavity filled with air which serves as both 1 by 4 power divider and mode splitter for dual polarization. Benefited from metal-only DMLS technology, two samples of complex configuration of antenna array are printed successfully, one using AISi10Mg powder and other using stainless steel as printing material. The schematic and fabricated prototype are shown in Fig. 20(a) and 20(b) respectively. The antenna array obtains gain of approximately 28.5 dBi respectively with the 90% radiation efficiency over the entire operating frequency band illustrated in Fig. 20(c).

Recently, [119] reported the new architecture for antenna arrays that solve constraints regarding wide scan bandwidth and high radiation efficiency of phased array antennas. The triangular lattice waveguide array is utilized with element based on 120° symmetry. The method reduces the effect of grating lobes and pre-excitations which enhance the radiation efficiency and scan angle while limiting the aperture size. Fig. 21(a) shows the schematic of Ku-band SATCOM phased array with tri-ridge aperture for LEO satellites. The fabricated prototype using AISi10Mg with

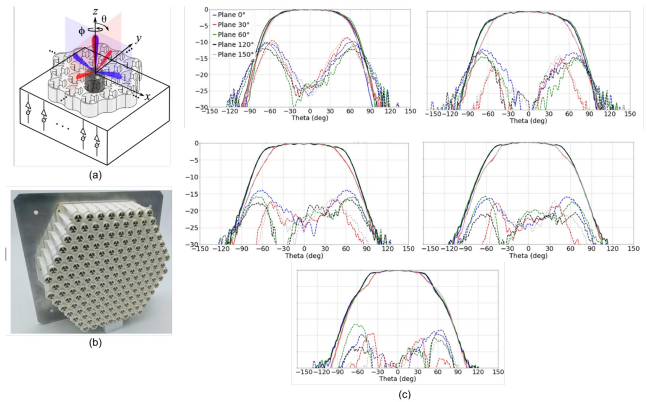


FIGURE 21. Tri-ridged antenna array, (a) Schematic view, (b) fabricated prototype, and (c) its beam scanning angles [119].

DMLS technology and further copper plating is used to enhance conductivity and surface finish shown in Fig. 21(b). The antenna array provided the gain of 4.5 to 6.3 dBi with return loss better than -10dB and achieve beam scanning of 360° over the different central frequencies of 10.7GHz, 11.2GHz, 11.7GHz, 12.2GHz and 12.7GHz respectively as given in Fig. 21(c).

In conclusion, SLM and DSM techniques are mostly adopted to manufacture antenna arrays for SATCOM. The simple slot antenna designs are recommended for high-gain millimeter-wave arrays when employing metal-based AM techniques [113], [114]. Aluminum alloys are particularly advantageous in this context, offering high gain and lower conductivity losses compared to stainless steel, making LPBF an efficient technology for modern SATCOM antenna array manufacturing [118]. The metal-based AM of antenna arrays is time-consuming process and faster production often incurred high cost which effects the large-scale production. The issue is due to conventional inclined-angle printing schemes used in AM which increased production time due to the need for additional layers in the vertical direction. By reducing the incline angle and distributing the metal powder horizontally significantly lowers production time. To apply proposed printing scheme along with self-supporting geometries, like pyramids and arc-shaped surfaces employed for component design, overall, 40% decrease in fabrication time is also observed in [118] without compromising structure accuracy and performance. Furthermore, lattice structure-based antenna array can also be realized using SLM technology which efficiently provide lightweight geometry with minimum surface roughness and high dimensional accuracy for onboard SATCOM [42].

B. AM RF COMPONENTS

The previous section has provided a thorough overview of the research done on AM antennas for SATCOM. However, apart from the antennas, it is essential that RF components can also be additively manufactured to realize fully-printed and monolithic SATCOM systems. In this regard, a great

TABLE 5. AM antenna arrays for Ku, K and Ka-band SATCOM.

Ref	Antenna Type	Technique	Material	Band	Gain (dBi)	Year
[121]	Active antenna array	DMLS	AlSi10Mg	Ku	14.7	2020
[122]	Tile based antenna	inkjet printing	Silver-nanoparticle ink	K	Not-defined	2022
[123]	Dielectric Resonator Antenna shared-aperture array	FDM	ABS	K/Ka	7(K-band) 10(Ka-band)	2022
[117]	4x4 Dual band, dual CP Antenna array using Gap waveguide	SLA	Resin	K/Ka	20.1(RHCP) 20.3(LHCP)	2022
[124]	CP monopulse antenna array	SLM	AlSi10Mg	Ka	32.2	2024

research effort has been made to realize standalone AM RF components, and as a following a brief discussion will be provided to highlight these works.

1) FILTERS

A filter is an essential component in wireless communications that allows the propagation of signals within a specific frequency band while highly attenuating, i.e., rejecting the signals from other bands. In the context of SATCOM applications, filters of a waveguide topology are of high interest due to its high quality factor, low loss and high power handling capability. A number of various AM waveguide filters have been reported in the literature for SATCOM applications at Ku, K, and Ka frequency bands.

One group of the reported works focus on developing band-pass filters by integrating waveguides with resonant structures of various shapes. For example, in [124], ellipsoidal resonators were used to implement a band-pass filter with a center frequency of 23.6 GHz and a relative bandwidth of 1%. It was realized using SLM of TA6V titanium alloy, followed by deposition of a silver via liquid chemical suspension (LiCS). A more advanced design - a triple-band filter for Ku band was designed in [125] through the use of cylindrical resonators arranged in an Olympic topology. A year later, the same authors [126] demonstrated that spherical resonators could improve the insertion loss and Q-factor of a triple-band filter, the prototype and S-parameters of which are shown in Fig. 22(a) and 22(b). Both these works utilized SLM for additive manufacturing, with the only difference being the choice of material: pure copper was used in [125], while AlSi10Mg was used in [126].

Another group of works used deformed cavities as a means of resonance, with a specific focus on enhancing out-of-band performance of the filters by controlling transmission zeros and suppressing parasitic modes. For instance, in [127] and [128], a filter based on deformed elliptical cavities was designed for passband operation between 13.6 and 16.5 GHz. The filter was fabricated using SLM of AlSi10M, with the fabricated prototype and performance metrics, indicating a relatively wide stopband, presented in Fig. 22(c) and 22(d). A more detailed discussion of the same design can be found in [129]. Two more passband filter designs utilizing cavity deformation approach were reported

in [130] (10.75-10.85 GHz) and [131] (13-14.8 GHz). These designs implemented deformed cavities within a circular and rectangular waveguides, respectively, and were both fabricated through SLM of AlSi10Mg.

Metamaterials have also been used to generate resonance within the waveguides. This approach was used in [134], [135], using meta-structures composed of pins integrated inside a rectangular waveguide. This design approach has led to miniaturized band-pass filters with a footprint decoupled from the operating frequency. For experimental validation, the filters were fabricated via SLM of AlSi10Mg for various passband widths.

Non-conventional waveguide designs have also been explored to design filters for SATCOM applications. For example, in [136], a groove gap waveguide structure was adopted to implement a low-pass filter with a maximum passband frequency of 36 GHz. The design was fabricated using SLM of AlSi10Mg, which was then followed by CNC milling to enhance the surface finish. In [132], a planar, rather than waveguide, topology was explored to design a band-pass filter (9.58-14.57 GHz), incorporating $\lambda/4$ resonators, capacitors and inductors. This work leveraged the flexibility of AM to produce a multilayer structure using simultaneous inkjet printing of conductive (silver) and dielectric materials. The resulting filter is compact and miniature, with the geometry and prototype shown in Fig. 22(e) and 22(f). Similarly, the flexibility of AM was explored in [133] to design a low-pass filter with a passband up to 16.3 GHz. This design not only provides filtering functionality, but also provides a mechanical twisting and H-plane bending, which are essential for highly integrated antenna solutions for SATCOM. This compact and multi-functional filter, shown in Fig. 22(g), 22(h), and 22(i), was fabricated through SLM of AlSi10Mg.

2) DIPLEXERS

AM filters facilitate implementing of AM diplexers - three port RF devices that split the incoming/outgoing signals into two frequency channels. In SATCOM systems, diplexers enable the use of a single antenna for both uplink and down-link operations while effectively separating and isolating the two channels. In [140], an AM diplexer with passband channels of 11.8-12.2 GHz and 13.4-14.2 GHz was realized

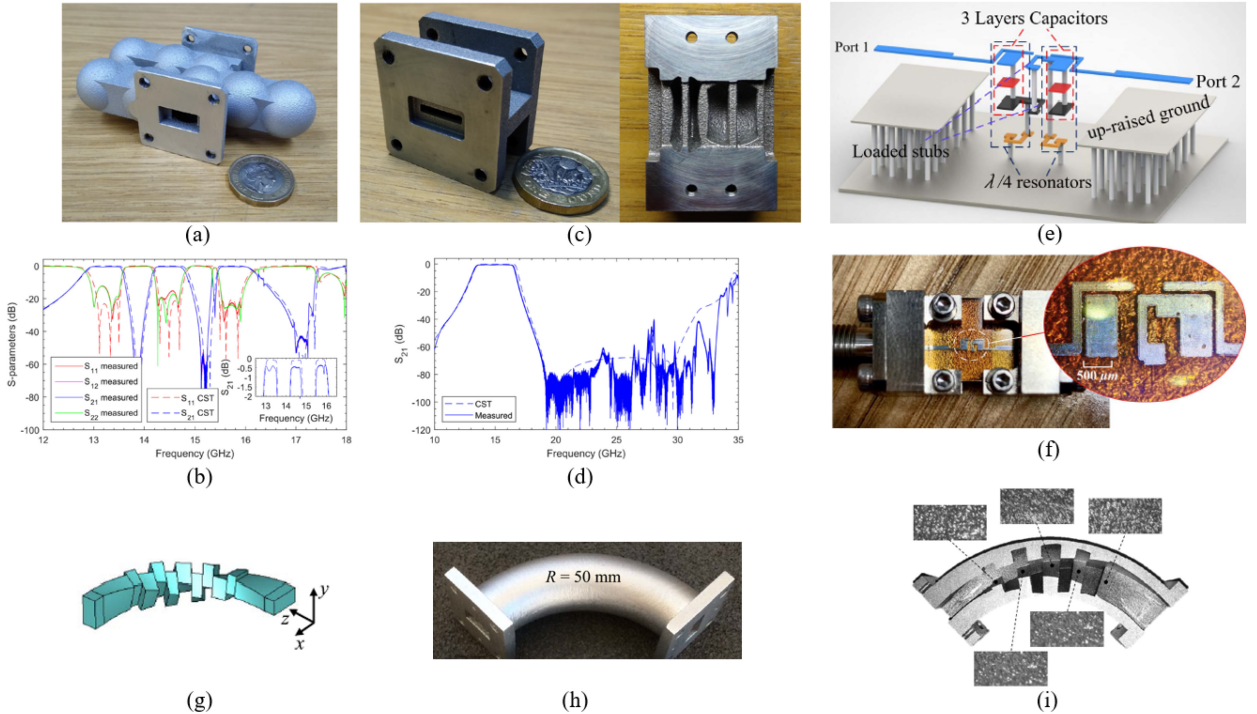


FIGURE 22. AM filters. (a) The triple-band waveguide filter proposed in [126] and (b) its S-parameters. (c) The pass-band filter with (d) wide stopband presented in [128]. (e) The geometry and (f) the fabricated prototype of the multilayer filter reported in [132]. (g) The internal structure, (h) the fabricated prototype along with (i) stereomicroscopic picture of the low-pass filter with bending and twisting functionalities proposed in [133].

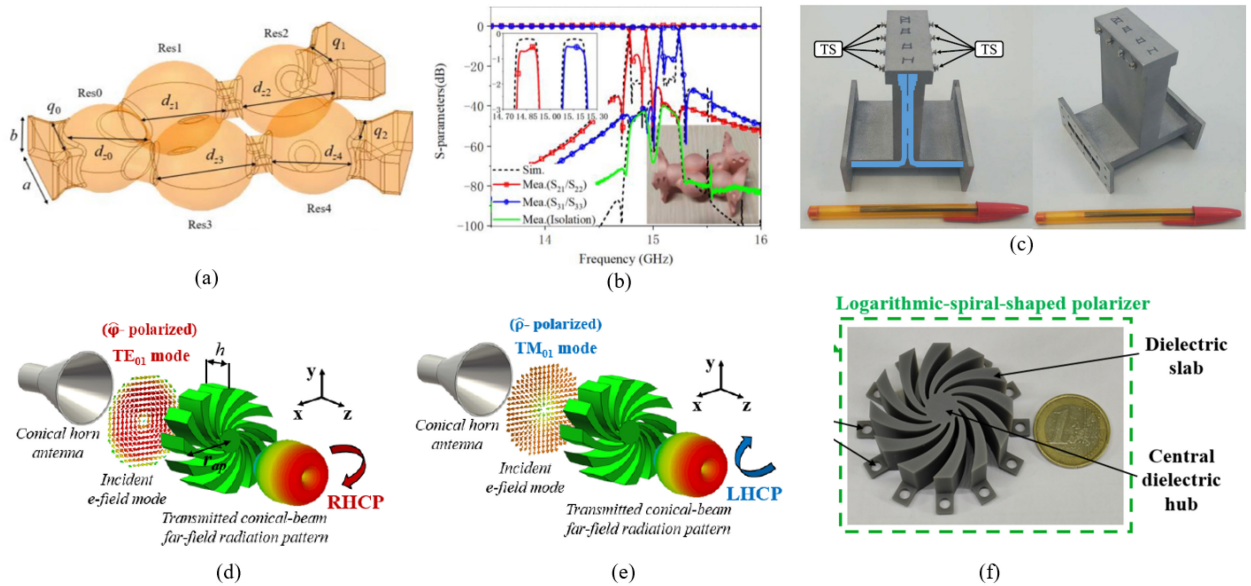


FIGURE 23. (a) The geometry of the diplexer proposed in [137] and (b) its S-parameters (fabricated prototype is shown in the inset). (c) The prototype of the phase shifter reported in [138]: this photo, in particular, demonstrates four phase shifters connected in parallel. (d), (e) The dual LP to dual CP polarizer proposed in [139] and (f) its fabricated prototype.

using FDM printing of the PLA and manual brushing of the silver. A more advanced fabrication approach sequentially incorporating SLA, chemical copper deposition, electrolytic copper and tin deposition was used in [141] to realize an AM diplexer with passbands of 13.7-14.7 GHz and 16.3-17.3 GHz. This work further incorporated a feeding network

that connected the diplexer to a 2 x 2 horn antenna array, all additively manufactured as a single monolithic block. In [142], an AM diplexer based on two pairs of band-pass filters, four 3 dB couplers and an H-bend was realized for two passband channels of 11.7-11.9 GHz and 12-12.3 GHz. For the fabrication, the authors relied on a combined AM



approach of Polyjet material jetting and FDM, followed by manual pouring of the silver paint for metallization. Alternatively, in [137], an AM diplexer with passbands of 14.8-14.93 GHz and 15.07-15.23 GHz was implemented using an all-resonator structure based on dimpled ellipsoid dual-mode resonators. This design, shown in Fig. 23(a) and 23(b), was fabricated through SLM of 4J36 invar alloy, which was then metallized by copper plating. The use of invar alloy provided high thermal stability - an important aspect for SATCOM - with the authors reporting only a 0.5 MHz shift in resonant frequency of the single resonators over a 100°C temperature variation.

3) PHASE SHIFTERS

Another crucial RF component is a phase shifter, which is a key device that facilitates electronic beam steering, a must feature of modern SATCOM antenna systems. Phase shifter is an active device, thus it requires a controllable medium for operation such as electrical, mechanical, magnetic etc. However, despite the importance of phase shifters for SATCOM applications, only two AM phase shifter designs have been identified in the literature [23], [138], where both of them have relied on mechanical actuation to induce phase shifting. The design proposed in [138], depicted in Fig. 23(c), utilizes a 90° hybrid waveguide coupler, with two of its ports reactively loaded with tuning screws. The prototype was fabricated through DLMS (of unspecified metal), and was measured to provide up to 270° of continuous phase shift at the center frequency of 17 GHz. Similarly, in [23], continuous phase shifting was achieved through a screw mechanism that loaded the waveguide with a dielectric insert. Slightly better performance was obtained in this work, with a maximum achieved phase shift of 270° at the same frequency of 17 GHz. This work employed Polyjet printing of VeroWhite resin to realize the main body of the waveguide, which was then metallized through copper electroplating, and FDM of ABS for the dielectric inserts.

4) POLARIZERS

As mentioned previously, CP antennas are essential for SATCOM applications to establish a communication link that is robust to environmental factors. However, designing and fabricating CP antennas is generally more challenging compared to LP antennas. One way to address this challenge is by using LP-to-CP polarizers. For example, in [143], DLMS of AlSi10Mg was used to realize a simple AM CP polarizer. The design is based on a coaxially-fed circular waveguide with two pairs of oppositely oriented internal grooves in its walls. The measurements indicate 3 dB axial ratio over a wide frequency range from 28 to 34 GHz. Alternatively, [139] presents a dielectric polarizer having a logarithmic spiral shape, that can convert radiation pattern of a conical horn antenna from dual LP to dual CP within 28 to 30 GHz. Fig. 23(d), (e) and (f) demonstrate the proposed design, which was fabricated through SLA of grey resin. In another work [144], a SLM of titanium was used to realize a

LP-to-CP polarizing screen. The design consists of a periodic structure made of 3-D cells that support the propagation of transverse electromagnetic (TEM) mode. This feature resulted in a wide frequency operation of the proposed polarizer ranging from 19.5 to 28.6 GHz.

5) MISCELLANEOUS

To implement complete AM antenna solutions for SATCOM, it is essential to develop and validate various other standalone AM RF components. A couple of works addressed these needs. For instance, in [145] an ON/OFF RF switch designed for operation in the K-band was developed using liquid metal for control. The proposed design is based on a waveguide that is printed through FDM of ABS. Notably, the same FDM printer was used to metallize the printed waveguide with silver. Two polytetrafluoroethylene (PTFE) tubes were embedded inside the waveguide, and microfluidic control was achieved by injecting a liquid metal, EGaIn, through the tubes. The switch is turned OFF when EGaIn fills the waveguide and turns ON when it is removed. In another work [146], a waveguide terminator suitable for operation between 17 and 20.5 GHz was designed for SATCOM. The prototype was fabricated through DMLS of AlSi10Mg, additionally requiring three stubs of absorbing material, Ecosorb MF-117, which were inserted after the main body was printed.

C. SUMMARY

In summary, it is evident that AM has unlocked a wide range of advantages in designing and manufacturing RF/antenna components for SATCOM. These include the ability of monolithic integration of components [35], [44], [48], reduce weight through optimal designs [42], [103], [107], and produce complex shapes [30], [42], [103], [118].

Through literature, these technologies have already proven its ability to design flexibility and integration that allowed fabrication of customized designs to meet the existing specifications of onboard SATCOM, including high gain, good radiation efficiency, wide bandwidth and good power-handling capabilities in reduced weight and size. But it's important to note that, despite the revolutionary potential of these developments, very few studies have explicitly investigated these components for onboard SATCOM systems. Only a smaller percentage have proved the performance of these components in the harsh space environment [33], [48], [105], [106], [109], [111], and [147].

Furthermore, most AM antennas acquire perforated structures to vary dielectric properties, reduce weight or introduce deployability by incorporating air gaps as in [63], [103], [104]. However, such perforated configuration of the antennas can significantly compromise their mechanical robustness and rigidity, leading to deformation under extreme mechanical stress during launch period. Therefore, perforated metamaterial structures must be optimally designed to retain functionality and strength while reducing weight. A good example is [66] which presents

an optimally designed perforated lens structure using QICO geometry that can withstand 456.18Kg weight force. Moreover, high-performance material selection with superior mechanical properties is also key to maintain mechanical integrity despite perforation.

Further research on advance antenna designs is necessary to fully realize the potential of AM for space application. That also entails improving the material qualities of printing substrates for increased radiation resistance, electrical conductivity, and thermal stability and carrying out performance validation tests such as vibration, thermal, vacuum environment and other space-like settings.

IV. CHALLENGES, ADVANCES, & FUTURE PROSPECTS IN AM OF ONBOARD SATELLITE RF/ANTENNA COMPONENTS

AM antenna/RF components must ensure longevity and performance reliability for onboard as well as ground terminal SATCOM. However, meeting onboard SATCOM requirements is significantly more challenging due to harsh space environment as well as strict launch and weight constraints. In contrast, adapting AM for ground-based SATCOM antennas is less constrained, but still influenced by several factors, including material durability, environmental challenges such as high humidity in coastal areas, notable temperature fluctuations, corrosion, mechanical stress and structural deformation caused by strong winds. Nevertheless, one can state that ground terminal requirements are generally less stringent compared to those of onboard terminal. Although these factors are not challenging to address for ground terminal. The AM for onboard SATCOM necessitates the evaluation of materials and AM techniques in terms of properties like mechanical strength, electrical and thermal conductivity of AM materials. This section provides a detailed discussion on space environmental challenges and improvements in material characteristics relevant to the AM of satellite components. It also highlights current advancements in AM technologies and address key technological challenges, such as thermal stability, surface roughness, multi-material printing and manufacturing precision, that impact the performance and reliability of onboard satellite RF/antenna components.

A. ATMOSPHERIC CHALLENGES

Table 6 summarizes the main challenges, including extreme temperature cycles, radiation exposure, thermal expansion, vacuum environment, and mechanical pressure, which affects the material characteristics and degrade the performance of onboard antenna/RF components. Before finalizing the prototype, it is necessary to evaluate intendant components in specialized chambers [148] specifically built to test designed prototype performance inside space atmosphere conditions. These chambers mimic harsh atmosphere characteristics to guarantee the performance and reliability of designed onboard satellite RF/antenna components in the real space environment.

B. AM MATERIAL CHALLENGES AND ADVANCEMENTS

In the manufacturing of satellite onboard antenna/RF components, materials used in manufacturing is critical choice because electromagnetic (EM) properties of material directly influence the performance of satellite components. Material used in AM are mainly divided into four categories polymers, ceramics, metals and composites. The composites are derived from combination of ceramic based polymer matrices, or by adding fillers to them. They are synthesized using different techniques to enhance electrical and mechanical properties of substrate used to print RF components. Table 7 entails the list of thermoplastics, ceramics, metal alloys and their composites commonly used in antenna/RF design.

It is important to note that electrical and mechanical properties of substrate material are important to realize as they directly influence the performance of RF devices. The electrical conductivity of material can be improved by using techniques like integrating conductive filler of carbon-based materials (multi-walls carbon nanotubes (MWCNTs), graphene or carbon black), hybrid fillers (combination of multiple conductive fillers), material blending, etc. with different AM materials. Furthermore, to enhance mechanical properties, techniques like carbon fiber-reinforcement is used in which a composite consists of matrix (base material such as polymers, ceramics etc) and fibers (carbon fiber (CF), glass fiber (GF), Basalt fiber (BF), and Kevlar fiber (KF)) combined together and produce high strength, low weight and durable composite material which also have specialized properties that can be altered according to the quantity of fiber and matrix used. Following to above mentioned characteristics, we will be realizing possible advancements available in literature regarding the suitability of substrate material for satellite antennas.

1) POLYMERS

Polymers have been appeared as frequently used material in AM of satellite antenna/RF components design because of their properties like lightweight, cost-efficient, and flexibility. Mostly polymers are thermoplastic having ability to soften on heat and harden on cooling, often during the printing process while maintaining inherent characteristics [151]. However, they mostly produce prototypes which are brittle in nature and exhibits low mechanical strength but recently polymer composites are developed which are highly adopted for producing antenna/RF components for SATCOM.

PLA is the thermoplastic polymer made from common crops like corn and cassava. It has several advantages like strength, low CET, and excellent stiffness along with low printing temperature. Besides all advantages it can be easily shatter upon physical stress, poor high-temperature, and impact resistance with quickly deformation as contact with high temperature. To overcome these defects, blending method is investigated to modify PLA mechanical properties, printing quality, and functional modification [152]. The authors investigated that by adding fillers, the tensile strength of PLA is improved. The fillers such as 10% of

**TABLE 6.** Space atmospheric challenges & mitigation strategies.

Challenges	Details	Effects on AM material	Possible Solutions	Degrees*	Ref
Extreme Temperature Cycle	Huge thermal cycle variation from very cold to high heat as satellite continuously orbits around the earth. LEO satellites experienced 9000 temperature cycles in one year	The extreme temperature cycle effects material, expands and contracts with temperature change, causing cracks and degrade the structure.	Using materials like polymers or metals that withstand temperature variation having suitable glass transition temperature (Tg) and thermal properties	-100 to +120 °C	[150]
Atmospheric Radiations	At the altitude of 300km from LEO the atmosphere contains radiations like atomic oxygen (AO) and solar UV radiations	Chemically and physically effects material causing erosion and deterioration	Coating of radiation-resistance layer; use of stable polymer or metal composites	VUV raidations: $\approx 10^{21}$ to 10^{22} photons/cm ² per year with intensity of 120-200 nm range. Electron energy level: 10keV to 1MeV per year. AO exposure: 2×10^{20} O-atoms/cm ² per year	[151]
Mechanical pressure	The pressure caused by satellite launch and in-orbit satellite movement	Can result in structural failure, particularly in AM components that are layer-based	Proper material selection and designed component undergoes vibration tests	Not-defined	—
Vacuum Environment	Free-space atmosphere results in outgassing and embrittlement in the material	Polymers absorb molecules and different gasses from air. Absence of atmosphere results in release of trapped gases that contaminate the free-space and affect equipment performance. It also reduces the flexibility over time.	Use AM materials that have low outgassing properties and component should undergo vacuum testing before finalization	No-defined	[151]

* all values are related to LEO orbit

calcined shell (CSh) increases the tensile strength from 29.81 ± 1.8 MPa to 49.06 ± 8.87 MPa [153] and adding 5% of poplar the strength reached to 60MPa [154]. Moreover, utilizing bioinspired carbon fiber (CF) rods in PLA resulted in three times higher tensile strength of 82.60MPa, the sample called as solid CF rod reinforced PLA [155]. Apart from tensile strength, CSh fillers also improve thermal stability. In [156], excellent thermal stability of approximately 200°C and increased in electrical conductivity was observed by adding propylene glycol (PPG) in filament composite consists of PLA matrix and MWCNT as filler. Another PLA composite called electrify, is a conductive filament consists of polyester as base matrix and copper as conductive filler embedded together and form a composite filament which results in enhanced electrical conductivity of approximately 60S/m. The elecctrifi conductive filament is also widely used to design antennas with higher gain and wider bandwidth compared to that of printed using pure PLA [157].

Another commonly used polymer is ABS, which also has the drawback of poor tensile strength, low impact resistance and easily deforms its shape when subjected to unfavorable environment conditions like thermal cycle variation, uneven temperature etc which limit its use in SATCOM. In [158] article, fiber reinforcing techniques like using short fibers reinforced samples of CF, GF and BF are investigated to improve physical properties of ABS. CF reinforcement provide high degree of improvement in tensile strength 60%, i.e., 76.12 ± 1.65 MPa and elastic modulus by 1.75 compared to GF, BF, and pure ABS. It is concluded that only the addition of CF filler notable increase the toughness. After discussing advancements in physical properties of ABS, in [159] to enhance the electrical conductivity, the 10 weight% of MWCNT filler combined into ABS matrix to form a nanocomposite which is than transforms into filament suitable for commercial FDM technology. Using this filament electrical conductivity of $232e^{-2}$ S/cm is achieved. In [160], author presented a highly effective synthesis process for ABS

TABLE 7. Mostly used materials in AM of RF/antenna components.

Materials	Type	Tg °C	CTE	Tensile strength (MPa)	ε	$\tan \delta$	UV radiation	AM technique
Acrylonitrile butadiene styrene (ABS) PREPERM ABS Polyether ether ketone (PEEK) Polycarbonate (PC) PC-ABS Polylactic acid (PLA) Nylon12 Polyetherimide (PEI)/Ultem Polyethylene terephthalate glycol (PeTG) Nylon (Polyamides (PA)) Poly-aryl ether ketones (PAEK) Polyetherketoneketone (PEKK)	Polymer	108-109	72μm/(mK)	30-60	2.6-3.30	0.025	Poor	
		210-240	N/a	28.0	2.5-12	0.0009	Good	
		143	2.6x10 ⁻⁵ in./in./°F	90-100	2.8-3.30	—	Good	
		120	3.9x10 ⁻⁵ in./in./°F (D696)	55-75	2.8-3.4	0.001-0.02 @0.001-10GHz	Medium-low	FDM
		125	4.10x10 ⁻⁵ in./in./°F	41	2.9 - 2.7	0.005-0.02	Moderate	
		55-60	41.0 μm/m.K	50	3.2	0.001	Low	
		150	50.0μm/m.K	50	3.098-3.215	0.018-0.023		
		180-220	3.1 μin/in/°F	104	2.9	0.0013 @ 1MHz	Medium	
		79-85	23.9-52.2 μin/in/°F	101	2.40-3.46 @ 1kHz	0.005	Low	
		40-70	90-95μm/m.K	84-90	3.2-3.8	0.02-0.03	Low	
Vero Photopolymer Resin	Polymer	150-158	47-108μm/m.K	110-199	3.48-3.74	0.0055	High	
		162	52.9μm/m°C	170	2.95	0.00363	High	
		58.0 50-150	55.8 μm / (m.C) 50-100μm/m °C	40-55 30-80	3.0 2.00-3.10	0.02 0.01-0.05	Low Medium-low	SLA
Epoxy Resin		15-220	55μm/m.K	90-120	3.4-6	0.02	Medium-low	
Hexagonal boron nitride E-Strate Aluminum Oxide (Al ₂ O ₃) La(Mg0.49Ca0.01Sn0.5)O ₃ Zirconium Tin Titanate(ZST) Silicoaluminum Carbonite(PDC-SiAlCN) Silicon Boron Carbonitride(SiBCN)	Ceramic	900	2.95μm/m°C	100GPa	4.0-4.4	0.00075-0.0018		
		1000	10.7 μm/m°C	248	23	0.001		
		1600	6.40 μm/m°C	69-665	9.8	0.0003	High	FDM/SLA
		1600	—	—	19.9	0.00012		
		2000	—	—	37	0.0002		
		1400	—	—	3.053	0.026		
		885	—	—	6.11	0.32		
		570	20μm/mK	450	—	—		
		427-816	17.2x10 μm/m°C	482	—	—	High	SLM/DMLS
		350	8.6-9.7x10μm/m°C	950	—	—		

copolymer also called ABS reduced graphene oxide (rGO) composites which provide improved mechanical strength, thermal and electrical conductivity. To achieve exceptional performance with low rGO content, the latex technology is used which has the ability to carefully distributes rGO around ABS microsphere resulting in continuous and uniform conductive network by using minimum rGO concentration. The process achieved an electrical conductivity of

0.09 S/m with only 0.062 vol% concentration of rGO. Castle et al. [161], proposed the formation of ABS composite by adding barium titanate (BaTiO₃) as filler in ABS and observed the improved relative permittivity as compared to pure ABS. Different concentration samples were tested and observed which concluded that 70wt% filler density enhanced the relative permittivity of composite material by 240%.

SATCOM and space industries are widely adopting polymer composites such as PEAK, PREPERM, PEEK and ULTEM (PEI) for AM of onboard antenna/RF components because they provide advantages like excellent mechanical strength, chemical and heat resistance, UV radiation resistance, minimum level of outgassing in vacuum and high thermal stability with good electrical properties [162]. For example, in Section III, authors in [109] uses PREPERM and fabricate dielectric RA for onboard SATCOM which showed excellent performance in harsh space environment. Also in [147] horn antenna was manufactured with low-cost FDM using PEKK for onboard SATCOM in low earth orbit (LEO). The type of polymer compound called Kapton from polyimide (PI) family is also widely used material in space environment [163] because it has UV radiation resistance, high tensile strength and withstand high temperature cycle typically from -269 to $+400$ C. It possesses good insulating characteristics, low dielectric constant and dissipation factor within wide range of temperature, ensuring performance stability [164]. Nevertheless, after six years Kapton degrade significantly in LEO due to extensive electrostatic discharge (ESD) and AO erosion. Initially a lot of techniques were used to mitigate PIs such as applying protective coatings, adding nanofillers, or three-dimensional graphene form (3D-C) combined as filler in the polyimide. 3D-C filler technique successfully protect polyimide with ESD present in space environment, but 3D-C/PI composite fail against AO exposure, which is dominant in LEO [164]. Therefore, authors in [164], used organic-inorganic hybrid, polyhedral oligomeric silsesquioxane (POSS) which has widely been used to improve properties of polymers and nanostructures carbon. Infusion of POSS in the PI surface increase material durability in an extensive AO environment and helps to improve thermal stability, mechanical strength, and chemical resistance of polymers.

2) CERAMICS

Ceramics are non-metallic, inorganic materials often divided into following categories: clays, cements, abrasives, glasses, and advance ceramics which are polycrystalline engineered to be used in different industrial application. Advance ceramics provide enhanced mechanical stability and wide range of dielectric permittivity with low dielectric loss at high frequencies as compared to polymers. They are vital for designing all-dielectric antenna and RF components structures such as lenses [70], [71], [72], dielectric resonator antennas [20], [165] and filters [166], [167]. These substrates are widely chosen because of their low CET, excellent mechanical stability, and high temperature resistance. Ceramic-based SLA (CSLA) AM technology is often used to print ceramic antennas. Many types of ceramic composite materials have been prepared in which resonant frequency have near-zero temperature coefficient, high quality factor and flexible control of the EM properties of material.

Moreover, further advancements in ceramics are also proposed which make them suitable for component design

for onboard SATCOM. For example, polymer derived ceramics (PDC) is a class of advanced ceramics in which a preceramic polymer undergoes a process called pyrolysis in which it is heated in a high temperature inert environment (usually argon or nitrogen) and transforms into ceramic [168]. The preceramic polymers include poly-organosiloxanes, polysilanzes, and polycarbonsilanes which leads to the production of silicon-based ceramics such as silicon carbide, silicon nitride, etc. and many other ceramics with enhance properties [169]. PDCs help to design complex structures with fine resolution along with ceramic fibers and protective coatings, which is challenging to obtain from advance ceramics. PDCs are better than many conventional ceramics because of their improved thermomechanical qualities. They do not degrade significantly when exposed to temperatures as high as 2000 °C in oxidizing environments. They have remarkable properties such as thermal durability and resistance to corrosion and harsh atmospheric conditions in space, which is important for satellite components onboard. The only drawback of PDC is during the transformation of polymer to ceramic using high-temperature, various gasses such as CO₂, H₂O, H₂ and CH₄ are realized causing huge mass loss which leads to 40% to 70% reduction in dimension of structure results in the formation of cracks and pores, hence it will be challenging to adopt it for large structural designs [170].

Despite many advantages of advance ceramics, they still suffer from brittle nature that lacks toughness and prone to sudden brittle failure which limit them from replacing more ductile metals. To overcome this, Ceramic Matrix Composites (CMCs) materials were developed using the carbon-fiber reinforcement method, in which ceramic fibers or nanoparticles are embedded in the ceramic matrix. Unlike PDC, CMCs are not processed using melting technique, but they are designed using sintering method like slurry infiltration, reactive melt infiltration, polymer infiltration and pyrolysis and chemical vapor infiltration [171]. However, ceramic composite powders are synthesized using methods like solid state route, pechini method, Sol-gel, laser synthesis, hydrothermal synthesis, melt synthesis and Coprecipitation route. CMCs also provide good thermal resistance and high mechanical strength. Apart from advancements in ceramic material, choice of AM technique also plays important role which is discussed in [172].

3) METAL AND IT'S ALLOYS

Metal AM is currently adopted for high performance antenna/RF component design because it provides lightweight and cost-efficient way to achieve performance such as high conductivity, tolerance and efficiency to UV radiation, along with durability and structural integrity. The materials used for metal AM are alloys of aluminum, carbon steel, stainless steel, and titanium. The most commonly used AM technology for metal printing are SLM and DMLS. In AM of onboard antenna/RF components metals can be

used in various forms such as metal powders, metal inks (conductive inks), metal sheets, metal coating, etc.

Although AM of all-metal structure provide great electrical conductivity and efficiency, but it lacks design precision because after production the material exhibits surface roughness which degrade the strength and overall performance of printed components. In [173] discussed mechanical properties of various metal AM structures and concluded that heat treatment in post-processing step may require to provide essential mechanical properties and helps to maintain performance. Mostly used metal-alloys are based on aluminum and silicon including AlSi7Mg and AlSi10Mg, have been widely used in AM of antenna/RF components [105], [111], [119]. These metal alloys suffered from residual stress after the manufacturing process due to rapid heating and cooling effect; that degrade the strength, dimensional stability, and durability of product. The study [174] shows that metal alloys properties such as electrical conductivity and mechanical strength were greatly influence by Si content in Al alloy. Optimizing Si concentration provide a trade-off between electrical conductivity and strength, allowing engineers to select the right content of Si based on the needs of required application. Moreover, heat treatment helped to change the mechanical properties of metal alloys based on specific uses such as reducing residual stress in structure that provide flexibility or ductility.

Additionally, AM metallic antenna/RF components design in [175], two different metals and corresponding AM technology were investigated to examine their future for microwave applications. The first metal was 361L stainless steel and second Cu-15Sn using the binder jetting and SLM AM techniques. The parameters such as surface roughness, fabrication tolerance, phases, and micro-structures were analyzed to examine the frequency limit of both metallic material and AM techniques. Furthermore, three types of post processing techniques for surface roughness were studied: gold electroplating, manual polish and micromachined process, out of them smooth surface was obtained by using micromachined process. The Cu-15Sn was softer, hence polishing was easier as compared to 316L stainless steel. The phases and micro-structures were analyzed to explore material content and how they impact overall performance of designed component. The demonstration of E, D, and H band horn antennas was successfully presented. All design prototypes achieved gain greater than 21.5dBi which shows the potential of metals and AM technique can be used for future SATCOM applications.

Like PMCs and CMCs, metal matrix composites (MMCs) are also available consists of fibers surrounded with a metal matrix. They provide good strength and stiffness along with temperature resistance superior to pure metal and PMCs. The use of MMCs is limited due to their heavy weight and high development cost. Various metallic matrix has been explored such as Al, Mg, Ti, Ni, Cu, Co, and Fe but aluminum (Al) matrix is widely used in MMCs. For reinforcement phase,

ceramic is used such as SiC, Al₂O₃, graphite etc. Metals have high electrical and thermal conductivity due to the presence of unbounded electrons. But problem arise when additional demand for high mechanical strength such as for onboard SATCOM is required. As alloying mechanism may increase the mechanical strength by introducing other metals like nickel or titanium to the base metal which ultimately improve the mechanical properties, but it gives arise to impurities which increases electrical resistivity thus reducing the conductivity. The impact of alloying leads to trade-off between electrical conductivity and mechanical strength. In recent years alternative techniques are introduced such as grain refinement, use of specific alloys (copper-chromium-zirconium CuCr1Zr) or composite materials [176].

4) SUMMARY

In summary, advance polymer composites such as PEEK, PREPERM, and ULTEM have already proved to be excellent substrate material for antenna/RF component designs used for onboard SATCOM [66], [91], [106], [109]. Together with AlSi10Mg metal alloy for direct metal printed structure discussed in [42], [105], [111], [119] and few ceramic composites specially for lens design analyzed in [70], [71], [72]. Nevertheless, innovations in composite materials and the incorporation of various fibers and fillers into polymer, ceramic and metal matrices have greatly contributed to rapid advancements in AM materials. Incorporating these elements, researchers have made considerable advances in the development of AM materials which possess improved electrical, mechanical, and thermal properties. These developments need further studies for their applicability in the design of high-performance RF/antenna components for onboard SATCOM. For instance, such polymer composites filled with ceramic particles can improve dielectric characteristics significantly, creating a wide span of dielectric constants effective in tuning EM responses. Further research is required in the development of AM materials that exhibit more diverse EM property profiles and high dielectric properties to realize miniaturized antenna with improved performances and excellent printability, because at higher frequencies the physical dimension of the component has a significant impact on the performance. Moreover, enhancing electrical conductivity using conductive fillers or inks such as carbon fillers, hybrid materials and using a blending method remains an important area for development. Further advancements in this area of research will be key in achieving high-performance AM-enabled RF/antenna components for future onboard SATCOM applications.

C. CHALLENGES IN AM TECHNOLOGIES

Although considerable progress has been achieved in the development of advanced materials specifically for AM usage in satellite RF/ antenna design, these advances alone will not result in efficient design. In order to fully realize AM potential in SATCOM, it is important to consider existing AM technological challenges and possible solution

considerations. As discussed above, the most widely used technologies in RF/antenna design are SLA, Polyjet, SLM, FDM, and DMLS. The AM technology encounters issues related to surface roughness, dimensional accuracy, resolution, multi-material and multi-object printing, and thermal stability. Table 8 shows the typical characteristic values for the above-mentioned AM technologies.

1) SURFACE ROUGHNESS

AM is layer-based technology which uses different types of polymers, ceramics, or metal powders to manufacture components. These types of material behave differently at different extreme temperatures, hence material type and machine precision greatly affect the surface finish of designed components. For example, liquid polymer resin print using SLA and Polyjet [106] or metal alloy print using SLM [35], often provide smooth surface finish. However, powdered form of polymer print using FDM [29] or metal powder print using DSM [48], encounter some surface roughness which greatly influence the performance in mm-wave. The SLA and Polyjet AM technologies use laser beam to cure the resin according to the design structure. Therefore, they both provide smooth surface finish as compared to other AM technologies. On the other side, FDM first uses heated nozzle to melt the filament and then deposit the melted filament on the building platform. It is cost-efficient technology but provide high surface roughness because of its inherent process characteristics and use materials like polymers or ceramics in solid form. Furthermore, Metal-based technologies like SLM and DMLS uses metal powder. SLM technology melts and solidifies all metal powder layer by layer using a high-power laser, producing a high-density metal prototype. The resulting products feature exceptional mechanical strength and surface smoothness due to the complete melting of powdered material while DMLS doesn't melt all metal powder, hence provide low surface finish as compared to SLM. It is suggested that using FDM and DMLS, machine optimization with some post-processing techniques can help to achieve acceptable surface finish in cost-efficient way [41], [101], [107].

2) RESOLUTION/ DIMENSIONAL ACCURACY

High resolution and dimensional accuracy are the common challenges in AM technologies, especially for complex design structures. Factors causing variations in intended dimensions may include thermal deformation, material shrinkage after cooling and fault in printing settings. SLA and Polyjet uses liquid resin hence their precision, flexibility and accuracy is better than other AM and vat polymerization methods such as digital light processing (DLP) and continuous digital light processing (CDLP) [177]. But they have high development cost with slow printing speed. Nevertheless, other technologies like FDM lacks dimensional accuracy and resolution. By selecting materials with low dielectric loss and optimizing print settings, such as layer height, nozzle diameter and temperature, FDM

can achieve a more refined surface finish and improved precision suggested in [101], [107], [109]. Additionally, post-processing techniques like polishing, coating, or vapor smoothing can further improve surface uniformity, making FDM a viable and cost-effective option for some high frequency applications. The SLM AM technology provides better mechanical properties, precision, and accuracy than other metal AM technologies. Unlike SLM, DMLS offers a cost-efficient and fast prototype manufacturing solution, which may affect surface quality and precision. Hence, both technologies play a significant role in metal-based AM antenna/RF component design for satellite communication. Therefore, when properties like high dimensional accuracy and surface finish with good mechanical strength in metal-based components are concerned, SLM is a better choice. If cost and speed are concerned DMLS can be used with some material pre-processing steps to obtain precision in dimensional accuracy.

3) MULTI-MATERIAL & MULTI-OBJECT PRINTING

Multi-material print brings many advantages like printing conductive and dielectric part together in single print which improve the performance by eliminating the assembly stage and related interference problem. On the other hand, multi-object printing is also important for fast prototyping, which is advantage for large-scale applications. However, in AM, materials are melted using a heated nozzle or in case of SLA, liquid form of material extrude from nozzle to form an object. Multi-material printing in a single cycle is challenging because properties like melting point, bonding capacity, viscosity, and density vary according to the material. The balance between these variations and design integrity can be challenging to maintain. Therefore, few AM techniques offer multi-material printing capabilities such as Polyjet, FDM, and DMLS while compromising final part performance. Multi-object printing depends on machine characteristics. Techniques like FDM, Polyjet, and DMLS also offer the advantage of multi-object printing at the same time but introduce issues like uniform material flow and heat management. Therefore, advanced techniques like hybrid manufacturing attempt to address these problems, as in [4], [23], [87], [178], but their applicability and scalability still need to be improved.

4) THERMAL STABILITY

Thermal stability depends on ability of material to retain its structural and mechanical characteristics under extreme temperature variation. Thermal instability in AM can lead to problems like cracking, warping and introduce residual stress during heating and cooling cycles. This is common in fusion-based technologies that often experience inconsistent heating and cooling effect such as FDM and SLM. For onboard SATCOM components, such thermal instabilities can degrade the longevity and reliability of antenna and RF components, potentially affecting the performance and structural durability in space environments.

TABLE 8. Characteristics of mostly used AM technologies in SATCOM.

Technology	Feedstock	Material Type	Dimensional Accuracy	Resolution	Quality of Surface Finish	Multi-material printing	Cost
SLA	UV-curable Liquid resin	Polymers, Ceramics, Composites	$\pm 0.2\%$	10-50 μm	High	No	High
Polyjet	UV-curable Liquid Resin	Polymers, Ceramics, Composites	$\pm 0.05\text{-}0.1\%$	5-16 μm	High	Yes	High
FDM	Filament	Polymers, polymer composites	$\pm 0.5\%$	50-200 μm	Low	Yes	Low
SLM	Powder	Metal, alloys, limited polymers & ceramics	$\pm 0.3\text{-}0.1\%$	50-100 μm	High	No	High
DMLS	Powder	Metal, alloys, limited polymers & ceramics	$\pm 0.2\%$	80-100 μm	Moderate	Yes	Low as compared to SLM

To mitigate these problems and guarantee reliable design performance, careful choice of material, post processing steps like post curing, and optimizing machine temperature can help to reduce airgaps and enhance thermal stability, ultimately improving the robustness of onboard SATCOM components.

5) FORMATION OF CAVITIES & LIMITED STRUCTURAL VOLUME

The formation of gaps between subsequent layers is one of the main problems with AM components. Improper layer bonding is one of the main reasons of void formation, which has an adverse effect on mechanical stability and performance of AM SATCOM components. For instance, gaps between layers may expand because of extrusion-based AM techniques like FDM or SLM which may cause delamination and unpredictable mechanical characteristics. However, pre-print settings such as properly heating the nozzle and bed along with proper post-curing may help to minimize the effect [179].

Furthermore, one of the biggest disadvantages of AM technology is its limited build capacity, which users usually experience. Massive parts are therefore typically reduced in size or broken down into smaller subcomponents, which takes more time and effort. Often, it is not feasible or efficient to scale down the model. In addition, the total strength of the subparts may be weakened using adhesives during assembly or use screws and connectors which make the prototype bulky. Ultimately, AM has yet long way to demonstrate satisfactory outcome in large-scale industrial applications [180].

D. ADVANCEMENTS IN AM TECHNOLOGIES

Currently, a large number of antenna/RF components for onboard satellite are still manufactured using conventional subtractive techniques such as CNC machining, electro-forming, or chemical etching [2], [3]. These techniques are used to fabricate horn antennas [181], reflectors, phased arrays [182], transmitarrays [2], reflectarrays [3], and waveguide networks [183] in split-blocks, which are typically assembled from multiple metal-parts. Despite their reliability, they still suffer from factors such as high cost, weight, limited design flexibility, material waste and long production time; therefore, AM-based antennas are promising to overcome these challenges. However, as summarized in Table 1, there are few constraints which limit the widespread adoption of AM technologies and materials for space applications. To bridge this gap, there is an urgent need in advance AM material, and AM processing techniques to produce onboard satellite antenna/RF components. In above sections, many techniques have been discussed to improve material quality by introducing composites, fillers and fibers. To process these composites, pre-processing techniques are necessary to overcome issues of nozzle blockage, porosity, thermal stability, and accuracy. Therefore, this section highlights advancements in AM technologies along with pre-processing ideas that can be further investigated for SATCOM. These developments, along with rigorous space qualification testing of components, are important breakthroughs to further enhance the feasibility of AM for space applications.

Direct Laser Writing (DLW) and Digital Light Processing (DLP) are important developments in AM for satellite antenna/RF components that need to be extremely precise. DLP is similar to SLA but cures complete layers at once by

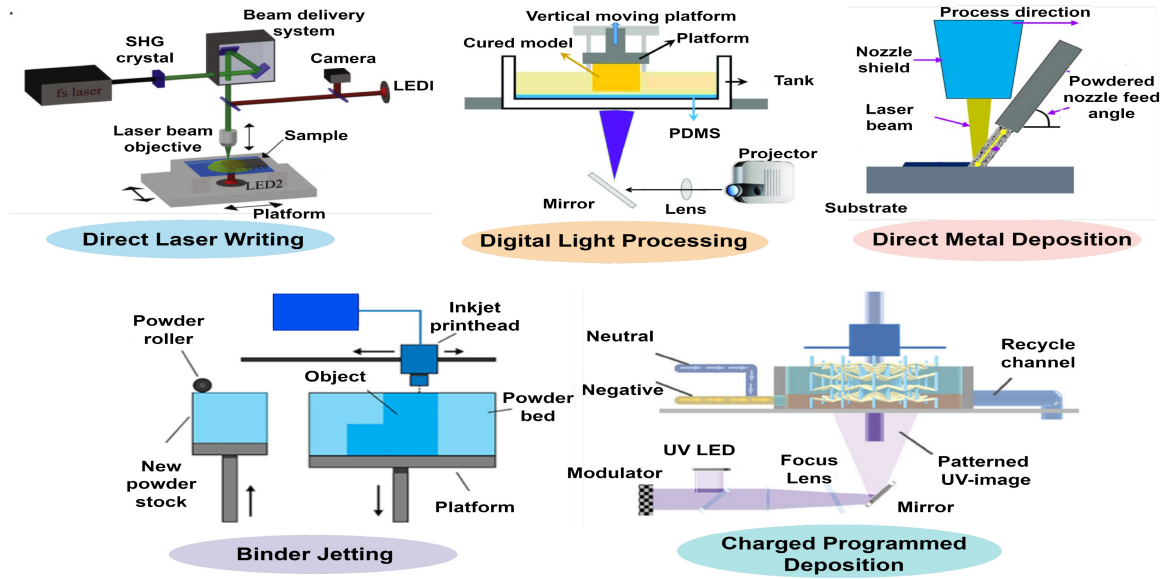


FIGURE 24. Advanced AM technologies [184], [185], [186], [187].

projecting a UV beam onto a resin surface using an electronic micro-mirror device shown in Fig. 24. This method works well to develop low-cost intricate, lightweight structures with excellent surface polish and dimensional accuracy, including high frequency satellite antenna/RF design [188]. However, DLW employs concentrated laser beams for nanometer accuracy, making it possible to fabricate complex micro-structural parts that are crucial to SATCOM systems shown in Fig. 24. Applications requiring high precision and high complicated geometry are best suited for these technologies such as in [189], [190] DLW is employed to print intricate geometry of high-frequency antennas and RF components for space applications.

The manufacturing of metallic and composite satellite components is being advanced via Direct Metal Deposition (DMD) and Binder Jet Printing (BJP) shown in Fig. 24. Satellite parts like antennae and RF components can be repaired or customized via DMD, which uses a laser or electron beam to melt and deposit powdered metal layer by layer. Because they can produce intricate, high-performance structures, DMD and BJT are very beneficial for designing antennas and RF components. Using conductive materials like copper or aluminum, DMD is excellent at producing dense, accurate metallic parts that are essential for effective component performance for SATCOM. Its ability to fabricate complex geometries, like waveguides or lattice structures, guarantees low losses and optimal signal transmission [191]. However, BJT is flexible and affordable, enabling the use of a wide range of materials, such as ceramics, metals, and composites which are perfect for adjusting the conductive and dielectric characteristics of RF devices. It is ideal for designing antenna arrays or parts for SATCOM due to its scalability and lightweight potential [192].

Another improvement in traditional SLA is MicroSLA, often achieves resolutions below a micron by modifying the photopolymerization technique to produce objects with micro- and nano-scale characteristics. MicroSLA uses specialized light-sensitive polymers and highly focused light sources (such as UV lasers beam or digitized micromirror technology) to produce complex geometries with remarkable accuracy and precision, in contrast to normal SLA, which is intended for macro-scale components. High frequency satellite antenna/ RF components which require high accuracy and miniaturization, can get benefit from this innovation [193], [194]. Charged Programmed Deposition (CPD) is becoming another more popular AM technique for manufacturing which involves microSLA to build the polymer structure with a programmable charged surface area and then using electric fields to regulate particle deposition as shown in Fig. 24. CPD enables accurate multi-material stacking, which is essential for satellite antennas, sensors and actuators [187]. For example, author in [195] utilized CPD printing process to fabricate complex metallic geometries without use of SLM or DMLS techniques. It results in lightweight monolithically antenna design using minimum steps. It involves two steps: firstly, polymer structure was developed with charged programmable surface area and then metal deposition was done to metalized charged surface area. The K-band horn antenna was successfully printed using CPD process and achieved gain of about 14.31 dBi over cut-off frequency of 19GHz and 80% of weight reduction without compromising the performance.

Some challenges regarding AM technology discussed in above section can be overcome by combining traditional AM methods with extra material pre-processing steps to improve printing quality of material with reduced void's formation between layers. Thus, enhancing strength and

durability of fabricated component. Such techniques include Electrophoretic Deposition (EPD), Selective Laser Gelation (SLG) and Plasma Laser Deposition Manufacturing (PLDM). PLDM improves thermal stability and lowers residual stress in high-performance satellite components by using plasma to warm or alter the surface of metal powders prior to laser fusion. It is the hybrid technology used to manufacture direct metal parts by combining conventional SLM and plasma to enhance the focused beam and melting process [196]. Similarly, EPD deposits nanoparticles onto materials using electric fields; the nanoparticles are then treated to improve the material's qualities. This technique is perfect for producing coatings with tailored conductivity or dielectric properties that are beneficial for multipurpose satellite parts. Selective laser gelation (SLG) is a recent development in hybrid layer fabrication. It blends the sol-gel process with the conventional selective laser sintering (SLS) method. The selective gelation procedure proven to be a promising method for creating highly precise ceramics and metal-ceramic composites components with exceptional surface finish. Additionally, cutting-edge techniques like Laser Surface Remelting (LSR) when combined with LPBF enhances the surface finish, relative density and minimize porosity, hence thermal conductivity is also improved [197]. Recently, in [198] article, protective gas (nitrogen and argon) was used using LSR to improve surface roughness, porosity, and complex microstructure of AlSi10Mg fabricated using LPBF.

V. CONCLUSION & FUTURE PERSPECTIVE

This review highlights the revolutionary potential of AM in design and manufacturing of antenna/RF components for SATCOM, specifically focused on Ku, K and Ka bands. AM techniques such as SLA, Polyjet, and SLM provide high dimensional accuracy and surface finish thus enabling the manufacturing of antennas/RF components having intricate complex inner or outer structure such as those miniaturized antennas for high frequency applications or printing grooves and ridges inside waveguides or horn antennas to improve wideband performance. All these benefits proved the flexibility to employ these AM techniques to design onboard SATCOM components. However, SLA and Polyjet are polymer and ceramic based techniques which successfully design dielectric part followed by metallization technique if required. Using these techniques, ceramic based designs of antenna/RF components print using SLA may considered more suitable for onboard SATCOM because they provide mechanical robustness with excellent wide range of dielectric permittivity. However, limited study has been provided which allows a path for further consideration. On the other hand, SLM is metal-based AM technique which successfully realize for onboard SATCOM components using metal-alloy called AlSi10Mg. Furthermore, FDM and DLSM technologies suffered from surface roughness and low dimensional accuracy therefore they are more considered for

ground terminal SATCOM applications within the context of literature available.

Advancements in materials, such as metal alloys composites, fiber-reinforced polymers, filler-added composites and PDCs have shown promising results in improving the mechanical, electrical, and thermal properties of AM-based components. This paper also emphasizes on recent developments in AM technologies and pre-processing methods aimed at addressing key challenges like porosity, improving resolution and accuracy, and ensuring stable thermal properties, factors crucial for the performance of onboard high-frequency component.

Future research should focus on development of advanced AM materials with improved EM properties and stable thermal characteristics. In particular, composite materials — synthesized by incorporating highly conductive fillers, fiber-reinforcement method or combining two different materials — shows great potential, as explored in this review and recently discussed in [199]. Moreover, it is important to consider the thermal expansion co-efficient of these materials, as they can significantly impact the performance and reliability of onboard AM-based antennas, depending on different orbit and environmental conditions

As highlighted in the review, AM offers great design flexibility for metallic [64], dielectric [69], and hybrid lens antennas [200]; should be explored further for future missions due to their compact structure, high gain, novel beam shaping, and beam scanning capabilities. The feasibility of AM for deployable antenna geometry is another compelling direction for onboard SATCOM due to strict size requirements in satellites. Incorporating perforated or lattice structures for mechanical deployability needs to be carefully engineered that withstands mechanical robustness as discussed in the review [66].

The investigation of metallization techniques is also critical research area, particularly those that can improve electrical conductivity and power handling capability while maintaining lightweight profile —essential for advancing the performance and reliability of AM-based onboard RF systems. One emerging approach worth exploring in this area is the incorporation of MXene-based materials for metallization. They provide excellent electrical conductivity without adding extra weight, making them ideal candidate for lightweight metallization for space components [201]. For example, in [202], [203] highlights the applicability of MXene for antenna and RF components. However, its reliability for onboard satellite use is yet to be fully realized.

Moreover, currently available research is focusing on filament-based AM of antennas and RF components, enabling direct metal printing of complex structures [204], [205]. However, these filaments have yet to be fully realized for SATCOM because of their low conductivity and mechanical strength. Further optimization of 3D printable filaments is required, ensuring their viability for high-performance space applications.



4D-AM printing is also emerging field that involves stimuli-responsive materials capable to adopt shape over time [206]. Incorporating smart materials opens new path for developing adaptive and reconfigurable antenna systems which are crucial for reliable SATCOM performance in dynamic space environments. Therefore, advanced study is advisable in 4D-AM of onboard SATCOM components.

To realize these advancements, optimization of AM methods is necessary. This includes preprocessing techniques together with improved or hybrid AM approach [23], [35], [92], [207] which can significantly improve precision and material quality of complex antenna geometries. However, limited research is currently available which required further investigation particularly for SATCOM components. Additionally, future study is also advisable on rigorous performance evaluation of AM antenna/RF components under space-like conditions, including vacuum environment testing, vibration testing, and thermal cycling, following standards given in [208] which provide standard procedure and environmental testing criteria to ensure equipment feasibility for onboard space applications.

Following the guidelines and research opportunities given in this review paper, AM will emerge as a transformative technology for realizing cost-effective, miniaturized, and lightweight onboard SATCOM components in the near future.

REFERENCES

- [1] C. A. Balanis, "Antenna theory: A review," *Proc. IEEE*, vol. 80, no. 1, pp. 7–23, Jan. 1992.
- [2] B. Shi et al., "Modular Ka-band transmit phased array antenna for SATCOM applications," in *Proc. IEEE 18th Eur. Conf. Antennas Propag. (EuCAP)*, 2024, pp. 1–5.
- [3] D. Martínez-de Rioja, E. Martínez-de Rioja, Y. Rodríguez-Vaqueiro, J. A. Encinar, and A. Pino, "Multibeam reflectarrays in Ka-band for efficient antenna farms onboard broadband communication satellites," *Sensors*, vol. 21, no. 1, p. 207, 2020.
- [4] F. Bongard, M. Gimersky, S. Doherty, X. Aubry, and M. Krummen, "3-D-printed Ka-band waveguide array antenna for mobile SATCOM applications," in *Proc. 11th Eur. Conf. Antennas Propag. (EUCAP)*, 2017, pp. 579–583.
- [5] Y. Yu et al., "Fully integrated design of a probe-fed open-ended waveguide filtering antenna using 3-D printing technology," *Int. J. RF Microw. Comput.-Aided Eng.*, vol. 31, no. 7, 2021, Art. no. e22680. [Online]. Available: <https://onlinelibrary.wiley.com/doi/abs/10.1002/mmce.22680>
- [6] M. Kalender, S. E. Kılıç, S. Ersoy, Y. Bozkurt, and S. Salman, "Additive manufacturing and 3-D printer technology in aerospace industry," in *Proc. 9th Int. Conf. Recent Adv. Space Technol. (RAST)*, 2019, pp. 689–694.
- [7] H. Bensoussan. "The history of 3-D printing: From the 80s to today. 3-D printing Blog: Tutorials, news, trends and resources." Accessed: Feb. 7, 2019. [Online]. Available: <https://www.google.com/search?q=H.+Bensoussan.+%282016.%29+The+History+of+3-D+Printing>
- [8] "History of 3-D printing: When was 3-D printing invented?" Feb. 2024. [Online]. Available: <https://all3-Dp.com/2/history-of-3-D-printing-when-was-3-D-printing-invented/>
- [9] "Inventor of FDM 3-D printing and co-founder of Stratasys, scott crump, inducted in to the TCT hall of fame." Sep. 2017. [Online]. Available: <https://investors.stratasys.com/news-events/press-releases/detail/418/inventor-of-fdm-3-D-printing-and-co-founder-of-stratasys>
- [10] K. Kanishka and B. Achterjee, "Revolutionizing manufacturing: A comprehensive overview of additive manufacturing processes, materials, developments, and challenges," *J. Manuf. Processes*, vol. 107, pp. 574–619, Dec. 2023. [Online]. Available: <https://www.sciencedirect.com/science/article/pii/S1526612523009726>
- [11] G. Gong et al., "Research status of laser additive manufacturing for metal: A review," *J. Mater. Res. Technol.*, vol. 15, pp. 855–884, Nov./Dec. 2021.
- [12] Y. Wang et al., "3-D printed antennas for 5G communication: Current progress and future challenges," *Chin. J. Mech. Eng. Additive Manuf. Front.*, vol. 2, no. 1, 2023, Art. no. 100065. [Online]. Available: <https://www.sciencedirect.com/science/article/pii/S2772665723000041>
- [13] B. Redwood, F. Schöffer, and B. Garret, *The 3-D Printing Handbook: Technologies, Design and Applications*, 3-D Hubs B.V., Amsterdam, The Netherlands, 2017. [Online]. Available: <https://books.google.lu/books?id=R3OvswEACAAJ>
- [14] A. D. Mazurchevici et al., "Additive manufacturing of composite materials by FDM technology: A review," *Indian J. Eng. Mater. Sci.*, vol. 27, no. 2, pp. 179–192, 2021.
- [15] M. B. De Leon et al., "3-D-printing for cube satellites (CubeSats): Philippines-perspectives," *Eng. Innov.*, vol. 1, pp. 13–27, Mar. 2022.
- [16] K. Rashed, "Ultra-performance polymer and composites in extrusion based additive manufacturing with space applications," Ph.D. dissertation, Dept. Comput. Sci., RMIT Univ., Melbourne, VIC, Australia, 2023.
- [17] D. Helena, A. Ramos, T. Varum, and J. N. Matos, "Antenna design using modern additive manufacturing technology: A review," *IEEE Access*, vol. 8, pp. 177064–177083, 2020.
- [18] J. S. Silva, M. Garcia-Vigueras, T. Debogović, J. R. Costa, C. A. Fernandes, and J. R. Mosig, "Stereolithography-based antennas for satellite communications in Ka-band," *Proc. IEEE*, vol. 105, no. 4, pp. 655–667, Apr. 2017.
- [19] F. Wang et al., "Stereolithographic additive manufacturing of Luneburg lens using Al₂O₃-based low sintering temperature ceramics for 5G MIMO antenna," *Additive Manuf.*, vol. 47, Nov. 2021, Art. no. 102244.
- [20] C. Morales, C. Morlaas, A. Chabory, R. Pascaud, M. Grzeskowiak, and G. Mazingue, "3-D-printed ceramics with engineered anisotropy for dielectric resonator antenna applications," *Electron. Lett.*, vol. 57, no. 18, pp. 679–681, 2021. [Online]. Available: <https://ietresearch.onlinelibrary.wiley.com/doi/abs/10.1049/el2.12234>
- [21] L. Polo-López et al., "Waveguide manufacturing technologies for next-generation millimeter-wave antennas," *Micromachines*, vol. 12, no. 12, p. 1565, 2021.
- [22] B. T. Malik, V. Doychinov, S. A. R. Zaidi, I. D. Robertson, and N. Somjit, "Antenna gain enhancement by using low-infill 3-D-printed dielectric lens antennas," *IEEE Access*, vol. 7, pp. 102467–102476, 2019.
- [23] S.-H. Shin et al., "Polymer-based 3-D printed ku-band steerable phased-array antenna subsystem," *IEEE Access*, vol. 7, pp. 106662–106673, 2019.
- [24] M. Li and Y. Yang, "Single-and multiple-material additively manufactured electronics: A further step from the microwave-to-terahertz regimes," *IEEE Microw. Mag.*, vol. 24, no. 1, pp. 30–45, Jan. 2023.
- [25] G. Richhariya, R. K. Shukla, M. Sawale, N. Vishwakarma, and N. Singh, "Recent trends in 3-D printing antennas," in *Array and Wearable Antennas*. Hoboken, NJ, USA: CRC Press, 2024, pp. 218–233.
- [26] J. Rao et al., "Advanced direct metal 3-D printed passive components for wireless communications and satellite applications," Ph.D. dissertation, Eng. Phys. Sci., Heriot-Watt Univ., Edinburgh, U.K., 2021.
- [27] S. K. Samal et al., "3-D-printed satellite brackets: Materials, manufacturing and applications," *Crystals*, vol. 12, no. 8, p. 1148, 2022.
- [28] O. A. Peverini et al., "Selective laser melting manufacturing of microwave waveguide devices," *Proc. IEEE*, vol. 105, no. 4, pp. 620–631, Apr. 2017.
- [29] M. E. Carkaci and M. Secmen, "The prototype of a wideband ku-band conical corrugated horn antenna with 3-D printing technology," *Adv. Electromagn.*, vol. 8, no. 2, pp. 39–47, Mar. 2019. [Online]. Available: <https://aemjournal.org/index.php/AEM/article/view/977>

- [30] I. Agnihotri and S. K. Sharma, "Design of a 3-D metal printed axial corrugated horn antenna covering full Ka-band," *IEEE Antennas Wireless Propag. Lett.*, vol. 19, no. 4, pp. 522–526, Apr. 2020.
- [31] N. Lee, C. Im, S. Park, and H. Choo, "Design of a metal 3-D printed double-ridged horn antenna with stable gain and symmetric radiation pattern over a wide frequency range," *IEEE Access*, vol. 11, pp. 100565–100572, 2023.
- [32] A. Sharma, R. K. Stilwell, S. Szczesniak, and C. Carpenter, "3-D metal printed Ka-band quad-ridge horn antenna," in *Proc. IEEE Int. Symp. Antennas Propag. USNC-USRI Radio Sci. Meeting (AP-S/USRI)*, 2022, pp. 1986–1987.
- [33] C. Stoumpos, J.-P. Fraysse, G. Goussetis, R. Sauleau, and H. Legay, "Quad-furcated profiled horn: The next generation highly efficient GEO antenna in additive manufacturing," *IEEE Open J. Antennas Propag.*, vol. 3, pp. 69–82, 2021.
- [34] W. Zhang et al., "3-D metal printed polarization reconfigurable horn antenna with solid & meshed structures: Future works for SATCOM applications," in *Proc. IEEE Int. Symp. Antennas Propag. North Amer. Radio Sci. Meeting*, 2020, pp. 1501–1502.
- [35] B. Zhang, R. Li, L. Wu, H. Sun, and Y.-X. Guo, "A highly integrated 3-D printed metallic K-band passive front end as the unit cell in a large array for satellite communication," *IEEE Antennas Wireless Propag. Lett.*, vol. 17, no. 11, pp. 2046–2050, Apr. 2018.
- [36] L. Alonso-González, J. Rico-Fernández, I. F. Vaquero, and M. Arrebola, "Metal-only additive-manufactured in monolithic piece array for sum/difference pattern in Ka-band," *IEEE Trans. Antennas Propag.*, vol. 71, no. 8, pp. 6413–6422, Aug. 2023.
- [37] Y. Li et al., "3-D printed high-gain wideband waveguide fed horn antenna arrays for millimeter-wave applications," *IEEE Trans. Antennas Propag.*, vol. 67, no. 5, pp. 2868–2877, May 2019.
- [38] M. Sabri, M. K. A Rahim, and F. Zubir, "3-D printed horn antenna using direct metal laser melting technique for millimetre wave applications," *Ind. J. Elect. Eng. Inf.*, vol. 7, no. 2, p. 78, May 2019.
- [39] K. V. Hoel, M. Ignatenko, S. Kristoffersen, E. Lier, and D. S. Filipovic, "3-D printed monolithic GRIN dielectric-loaded double-ridged horn antennas," *IEEE Trans. Antennas Propag.*, vol. 68, no. 1, pp. 533–539, Jan. 2020.
- [40] L. Wu, C. Wang, S. Peng, and Y. Guo, "3-D printed wideband millimeter-wave horn antenna with conical radiation pattern," *IEEE Antennas Wireless Propag. Lett.*, vol. 19, no. 3, pp. 453–456, Mar. 2020.
- [41] F. Filice et al., "3-D printed high-efficiency wideband 2×2 and 4×4 double-ridged waveguide antenna arrays for ku-band Satcom-on-the-move applications," in *Proc. 14th Eur. Conf. Antennas Propag. (EuCAP)*, 2020, pp. 1–5.
- [42] P. Lyu, X. Ma, W. Wang, J. Yang, Y. Li, and H. Zhang, "3-D printed lattice structure for lightweight Ka-band phased array antenna," *Electron. Lett.*, vol. 57, no. 23, pp. 863–864, Aug. 2021.
- [43] S. Azman and M. F. bin Mansor, "3-D printed dielectric rod antenna for ku-band frequency operation," in *Proc. 26th IEEE Asia-Pac. Conf. Commun. (APCC)*, 2021, pp. 281–285.
- [44] J. Zhang, X. Li, Z. Qi, Y. Huang, and H. Zhu, "Dual-band dual-polarization horn antenna array based on orthomode transducers with high isolation for satellite communication," *IEEE Trans. Antennas Propag.*, vol. 70, no. 10, pp. 9247–9259, Oct. 2022.
- [45] L. Alonso-González, J. Rico-Fernández, A. F. Vaquero, and M. Arrebola, "Millimeter-wave lightweight 3-D-printed 4×1 aluminum array antenna," in *Proc. 16th Eur. Conf. Antennas Propag. (EuCAP)*, Mar. 2022, pp. 1–5. [Online]. Available: <https://ieeexplore.ieee.org/document/9768999/>
- [46] E. Calà, M. Baldelli, A. Catalani, E. Menargues, G. Toso, and P. Angeletti, "Development of a Ka-band non-regular multibeam coverage antenna," *IEEE Trans. Antennas Propag.*, vol. 71, no. 1, pp. 7–17, Jan. 2023.
- [47] Y. D. Zárate, F. Torres, M. Rodriguez, and F. Pizarro, "3-D-printed low-cost choke corrugated Gaussian profile horn antenna for Ka-band," *Sci. Rep.*, vol. 13, no. 1, Dec. 2023, Art. no. 22957. [Online]. Available: <https://doi.org/10.1038/s41598-023-50174-5>
- [48] P. Vaitukaitis, J. Rao, K. Nai, and J. Hong, "Design of integrated wideband WR34-band diplexer-antenna array module for exploration of monolithic metal 3-D printing for space applications," *IET Microw. Antennas Propag.*, vol. 18, no. 4, pp. 280–290, 2024. [Online]. Available: <https://ietresearch.onlinelibrary.wiley.com/doi/abs/10.1049/mia2.12468>
- [49] A. I. Dimitriadis et al., "Polymer-based additive manufacturing of high-performance waveguide and antenna components," *Proc. IEEE*, vol. 105, no. 4, pp. 668–676, Jun. 2017.
- [50] S. Sirci, E. Menargues, and M. Billod, "Space-qualified additive manufacturing and its application to active antenna harmonic filters," in *Proc. IEEE MTT-S Int. Microw. Filter Workshop (IMFW)*, 2021, pp. 239–242.
- [51] E. Merchand, *Gradient Index Optics*. Amsterdam, The Netherlands: Elsevier, 2012.
- [52] I. Munina, I. Grigoriev, G. O'donnell, and D. Trimble, "A review of 3-D printed gradient refractive index lens antennas," *IEEE Access*, vol. 11, pp. 8790–8809, 2023.
- [53] Q.-W. Lin and H. Wong, "A low-profile and wideband lens antenna based on high-refractive-index metasurface," *IEEE Trans. Antennas Propag.*, vol. 66, no. 11, pp. 5764–5772, Nov. 2018.
- [54] J. M. Poyanco, F. Pizarro, and E. Rajo-Iglesias, "3-D-printed half-maxwell fish-eye dielectric lens antenna with integrated DRA feed," in *Proc. 16th Eur. Conf. Antennas Propag. (EuCAP)*, 2022, pp. 1–5.
- [55] A. Piroutiniya et al., "Beam steering 3-D printed dielectric lens antennas for millimeter-wave and 5G applications," *Sensors*, vol. 23, no. 15, p. 6961, 2023. [Online]. Available: <https://www.mdpi.com/1424-8220/23/15/6961>
- [56] Z. Larimore, S. Jensen, A. Good, A. Lu, J. Suarez, and M. Mirotznik, "Additive manufacturing of Luneburg lens antennas using space-filling curves and fused filament fabrication," *IEEE Trans. Antennas Propag.*, vol. 66, no. 6, pp. 2818–2827, Jun. 2018.
- [57] D. Jia, Y. He, N. Ding, J. Zhou, B. Du, and W. Zhang, "Beam-steering flat lens antenna based on multilayer gradient index metamaterials," *IEEE Antennas Wireless Propag. Lett.*, vol. 17, no. 8, pp. 1510–1514, Aug. 2018.
- [58] M. Herzberger and R. V. Mises, *Mathematical Theory of Optics*. Berkeley, CA, USA: Univ. California Press, 1945.
- [59] Z. Wang, K. Fan, and G. Q. Luo, "Millimeter-wave dual circularly polarized multibeam antenna array based on 3-D-printed Luneburg lens," in *Proc. IEEE Int. Workshop Radio Freq. Antenna Technol. (iWRF&AT)*, 2024, pp. 61–63.
- [60] O. Björkqvist, O. Dahlberg, and O. Quevedo-Teruel, "Additive manufactured three dimensional Luneburg lens for satellite communications," in *Proc. 13th Eur. Conf. Antennas Propag. (EuCAP)*, 2019, pp. 1–4.
- [61] Y. Li, L. Ge, M. Chen, Z. Zhang, Z. Li, and J. Wang, "Multibeam 3-D-printed Luneburg lens fed by magnetoelectric dipole antennas for Millimeter-wave MIMO applications," *IEEE Trans. Antennas Propag.*, vol. 67, no. 5, pp. 2923–2933, May 2019.
- [62] B. Qu, S. Yan, A. Zhang, F. Wang, and Z. Xu, "3-D printed cylindrical Luneburg lens for dual polarization," *IEEE Antennas Wireless Propag. Lett.*, vol. 20, no. 6, pp. 878–882, Jun. 2021.
- [63] C. Wang, J. Wu, and Y.-X. Guo, "A 3-D-printed wideband circularly polarized parallel-plate Luneburg lens antenna," *IEEE Trans. Antennas Propag.*, vol. 68, no. 6, pp. 4944–4949, Jun. 2020.
- [64] J. Rico-Fernández, F. V. Vidarsson, M. Arrebola, N. J. G. Fonseca, and O. Quevedo-Teruel, "Compact and lightweight additive manufactured parallel-plate waveguide half-Luneburg geodesic lens multiple-beam antenna in the K\$_{\{\alpha\}}\$-band," *IEEE Antennas Wireless Propag. Lett.*, vol. 22, no. 4, pp. 684–688, Apr. 2023. [Online]. Available: <https://ieeexplore.ieee.org/document/9950611/>
- [65] N. J. Fonseca, Q. Liao, and O. Quevedo-Teruel, "Compact parallel-plate waveguide half-Luneburg geodesic lens in the Ka-band," *IET Microw. Antennas Propag.*, vol. 15, no. 2, pp. 123–130, 2021.
- [66] C. Wang, J. Wu, and Y.-X. Guo, "A 3-D-printed multibeam dual circularly Polarized Luneburg lens antenna based on quasi-icosahedron models for Ka-band wireless applications," *IEEE Trans. Antennas Propag.*, vol. 68, no. 8, pp. 5807–5815, Aug. 2020.
- [67] S. Biswas et al., "Realization of modified Luneburg lens antenna using quasi-conformal transformation optics and additive manufacturing," *Microw. Opt. Technol. Lett.*, vol. 61, no. 4, pp. 1022–1029, 2019.
- [68] J.-M. Poyanco, F. Pizarro, and E. Rajo-Iglesias, "3-D-printed dielectric GRIN planar wideband lens antenna for 5G applications," in *Proc. 15th Eur. Conf. Antennas Propag. (EuCAP)*, 2021, pp. 1–4.
- [69] J.-M. Poyanco, F. Pizarro, and E. Rajo-Iglesias, "Cost-effective wideband dielectric planar lens antenna for millimeter wave applications," *Sci. Rep.*, vol. 12, no. 1, p. 4204, Mar. 2022. [Online]. Available: <https://doi.org/10.1038/s41598-022-07911-z>



- [70] Y.-H. Lou et al., "Design of ku-band flat Luneburg lens using ceramic 3-D printing," *IEEE Antennas Wireless Propag. Lett.*, vol. 20, no. 2, pp. 234–238, Jan. 2021.
- [71] F. Wang et al., "Stereolithographic additive manufacturing of Luneburg lens using Al2O3-based low sintering temperature ceramics for 5G MIMO antenna," *Additive Manuf.*, vol. 47, Nov. 2021, Art. no. 102244. [Online]. Available: <https://www.sciencedirect.com/science/article/pii/S2214860421004048>
- [72] Y. Lou et al., "Fabrication of high-performance MgTiO₃–CaTiO₃ microwave ceramics through a stereolithography-based 3-D printing," *Ceramics Int.*, vol. 46, no. 10, pp. 16979–16986, 2020. [Online]. Available: <https://www.sciencedirect.com/science/article/pii/S0272884220309329>
- [73] I. Grigoriev and I. Munina, "Multibeam truncated Gutman lens based on additive manufacturing," in *Proc. Int. Workshop Antenna Technol. (iWAT)*, 2022, pp. 104–106.
- [74] O. Bjorkqvist, O. Zetterstrom, and O. Quevedo-Teruel, "Additive manufactured dielectric Gutman lens," *Electron. Lett.*, vol. 55, no. 25, pp. 1318–1320, 2019. [Online]. Available: <https://ietresearch.onlinelibrary.wiley.com/doi/abs/10.1049/el.2019.2483>
- [75] B. C. Chen, Y. M. Pan, and S. Y. Zheng, "Truncated 2-D Gutman lens antenna with planar feeding surface for stable wide-angle beam scanning in millimeter-wave band," *IEEE Trans. Antennas Propag.*, vol. 71, no. 11, pp. 9030–9035, Nov. 2023.
- [76] K. H. Jeong and N. Ghalichechian, "3-D-printed 4-zone Ka-band fresnel lens: Design, fabrication, and measurement," *IET Microw. Antennas Propag.*, vol. 14, no. 1, pp. 28–35, 2020.
- [77] G.-B. Wu, Y.-S. Zeng, K. F. Chan, S.-W. Qu, and C. H. Chan, "3-D printed circularly polarized modified fresnel lens operating at terahertz frequencies," *IEEE Trans. Antennas Propag.*, vol. 67, no. 7, pp. 4429–4437, Jul. 2019.
- [78] J. Zhu et al., "Additively manufactured millimeter-wave dual-band single-polarization shared aperture fresnel zone plate metalens antenna," *IEEE Trans. Antennas Propag.*, vol. 69, no. 10, pp. 6261–6272, Oct. 2021.
- [79] K. H. Jeong, "Design, fabrication and measurement of Millimeter fresnel lens and helical antenna using additive manufacturing," M.S. thesis, Dept. Comput. Sci., Ohio State Univ., Columbus, OH, USA, 2017.
- [80] R. Rudduck and C. Walter, "Luneberg lenses for space communications," *IRE Trans. Space Electron. Telemetry*, vol. SET-8, no. 1, pp. 31–38, Mar. 1962.
- [81] J. Y. Li and M. N. M. Kehn, "The 90° rotating Eaton lens synthesized by metasurfaces," *IEEE Antennas Wireless Propag. Lett.*, vol. 17, no. 7, pp. 1247–1251, Jul. 2018.
- [82] M. Chen, O. Habiboglu, F. Mesa, and O. Quevedo-Teruel, "Ray-tracing and physical-optics model for planar Mikaelian lens antennas," *IEEE Trans. Antennas Propag.*, vol. 72, no. 2, pp. 1735–1744, Feb. 2024.
- [83] W. Shao and Q. Chen, "Single-pixel scanning near-field imaging with subwavelength resolution using sharp focusing Mikaelian lens," *IEEE Trans. Microw. Theory Techn.*, vol. 71, no. 2, pp. 795–804, Feb. 2022.
- [84] J. Chen, S. X. Huang, K. F. Chan, G.-B. Wu, and C. H. Chan, "A hybrid lens to realize electrical real-time super-resolution imaging," *Laser Photon. Rev.*, vol. 18, no. 11, 2024, Art. no. 2400263.
- [85] S. Zhang, P. Liu, and W. Whittow, "Design and fabrication of 3-D-printed high-gain broadband fresnel zone lens using hybrid groove-perforation method for Millimeter-wave applications," *IEEE Antennas Wireless Propag. Lett.*, vol. 21, no. 1, pp. 34–38, Jan. 2022.
- [86] B. Zhang et al., "A K-band 3-D printed focal-shifted two-dimensional beam-scanning lens antenna with nonuniform feed," *IEEE Antennas Wireless Propag. Lett.*, vol. 18, no. 12, pp. 2721–2725, Dec. 2019.
- [87] J. Monkevich and G. Le Sage, "Design and fabrication of a custom-dielectric fresnel multi-zone plate lens antenna using additive manufacturing techniques," *IEEE Access*, vol. 7, pp. 61452–61460, 2019.
- [88] J.-M. Poyanco, F. Pizarro, and E. Rajo-Iglesias, "3-D-printing for transformation optics in electromagnetic high-frequency lens applications," *Materials*, vol. 13, no. 12, p. 2700, 2020. [Online]. Available: <https://www.mdpi.com/1996-1944/13/12/2700>
- [89] S. Alkaraki, Y. Gao, S. Stremdsøerfer, E. Gayets, and C. G. Parini, "3-D printed corrugated plate antennas with high aperture efficiency and high gain at X-band and Ka-band," *IEEE Access*, vol. 8, pp. 30643–30654, 2020.
- [90] A. Papathanasiopoulos, J. Budhu, Y. Rahmat-Samii, R. E. Hodges, and D. F. Ruffatto, "3-D-printed shaped and material-optimized lenses for next-generation spaceborne wind scatterometer weather radars," *IEEE Trans. Antennas Propag.*, vol. 70, no. 5, pp. 3163–3172, May 2022.
- [91] K. Trzebiatowski, W. Kalista, M. Rzymowski, U. Kulas, and K. Nyka, "Multibeam antenna for Ka-band CubeSat connectivity using 3-D printed lens and antenna array," *IEEE Antennas Wireless Propag. Lett.*, vol. 21, no. 11, pp. 2244–2248, Nov. 2022.
- [92] Y. Kim, R. Phon, E. Park, and S. Lim, "An additively manufactured deployable broadband metasurface lens antenna," *IEEE Antennas Wireless Propag. Lett.*, vol. 22, no. 7, pp. 1672–1676, Jul. 2023.
- [93] B. Z. B. Xu, "A compact 3-D printed mirror folded lens antenna for 5G applications," *Progr. Electromagn. Res. C*, vol. 131, pp. 35–48, Dec. 2023.
- [94] A. Bansal, C. J. Panagamuwa, and W. G. W. A. S. Smieee, "Novel design methodology for 3-D-printed lenses for traveling wave antennas," *IEEE Open J. Antennas Propag.*, vol. 4, pp. 196–206, 2023.
- [95] B. Xu, B. Zhang, and X. An, "A 3-D printed low-profile wideband circularly polarized elliptical integrated lens antenna," *IET Microw. Antennas Propag.*, vol. 18, no. 4, pp. 272–279, Apr. 2024.
- [96] N. Melouki et al., "3-D-printed conformal meta-lens with multiple beam-shaping functionalities for mm-wave sensing applications," *Sensors*, vol. 24, no. 9, p. 2826, 2024. [Online]. Available: <https://www.mdpi.com/1424-8220/24/9/2826>
- [97] B. Imaz-Lueje, D. R. Prado, M. Arrebola, and M. R. Pino, "Reflectarray antennas: A smart solution for new generation satellite mega-constellations in space communications," *Sci. Rep.*, vol. 10, no. 1, 2020, Art. no. 21554.
- [98] B. Li, P. F. Jing, L. Q. Sun, K. W. Leung, and X. Lv, "3-D printed OAM reflectarray using half-wavelength rectangular dielectric element," *IEEE Access*, vol. 8, pp. 142892–142899, 2020.
- [99] P. Mei, S. Zhang, and G. F. Pedersen, "A wideband 3-D printed reflectarray antenna with mechanically reconfigurable polarization," *IEEE Antennas Wireless Propag. Lett.*, vol. 19, no. 10, pp. 1798–1802, Oct. 2020.
- [100] B. Li, C. Y. Mei, Y. Zhou, and X. Lv, "A 3-D-printed wideband circularly polarized dielectric reflectarray of cross-shaped element," *IEEE Antennas Wireless Propag. Lett.*, vol. 19, no. 10, pp. 1734–1738, Oct. 2020.
- [101] Y.-X. Sun, D. Wu, and J. Ren, "Millimeter-wave dual-polarized dielectric resonator reflectarray fabricated by 3-D printing with high relative permittivity material," *IEEE Access*, vol. 9, pp. 103795–103803, 2021.
- [102] J. Zhu, Y. Yang, D. Megloin, S. Liao, and Q. Xue, "3-D printed all-dielectric dual-band broadband reflectarray with a large frequency ratio," *IEEE Trans. Antennas Propag.*, vol. 69, no. 10, pp. 7035–7040, Oct. 2021.
- [103] Y. Cui, R. Bahr, S. A. Nauroze, T. Cheng, T. S. Almoneef, and M. M. Tentzeris, "3-D printed 'Kirigami'-inspired deployable bi-focal beam-scanning dielectric reflectarray antenna for mm-Wave applications," *IEEE Trans. Antennas Propag.*, vol. 70, no. 9, pp. 7683–7690, Sep. 2022.
- [104] Q. Cheng et al., "Dual circularly polarized 3-D printed broadband dielectric reflectarray with a linearly polarized feed," *IEEE Trans. Antennas Propag.*, vol. 70, no. 7, pp. 5393–5403, Jul. 2022.
- [105] J. Zhu, S. Liao, and Q. Xue, "3-D printed millimeter-wave metal-only dual-band circularly polarized reflectarray," *IEEE Trans. Antennas Propag.*, vol. 70, no. 10, pp. 9357–9364, Oct. 2022.
- [106] A. Palomares-Caballero, C. Molero, P. Padilla, M. Garcia-Viguera, and R. Gillard, "Wideband 3-D-printed metal-only reflectarray for controlling orthogonal linear polarizations," *IEEE Trans. Antennas Propag.*, vol. 71, no. 3, pp. 2247–2258, Mar. 2023.
- [107] A. Massaccesi et al., "Three-dimensional-printed wideband perforated dielectric-only reflect-array in Ka-band," *IEEE Trans. Antennas Propag.*, vol. 71, no. 10, pp. 7848–7859, Oct. 2023.

- [108] S. Tiwari, A. K. Singh, and A. Dubey, "Additively manufactured dielectric reflect-array antenna for Millimeter-wave satellite communication," *IEEE Antennas Wireless Propag. Lett.*, vol. 23, no. 4, pp. 1276–1280, Apr. 2024. [Online]. Available: <https://ieeexplore.ieee.org/document/10384695/>
- [109] S. Tiwari, A. K. Singh, and A. Dubey, "Additively manufactured dielectric reflectarray antenna for Millimeter wave satellite communication," *IEEE Antennas Wireless Propag. Lett.*, vol. 23, no. 4, pp. 1276–1280, Apr. 2024.
- [110] W. Feury et al., "Evaluation of metal coating techniques up to 66 GHz and their application to additively manufactured bandpass filters," in *Proc. 47th Eur. Microw. Conf. (EuMC)*, 2017, pp. 512–515.
- [111] J. Zhu, S. Liao, S. Li, and Q. Xue, "Additively manufactured metal-only millimeter-wave dual circularly polarized reflectarray antenna with independent control of polarizations," *IEEE Trans. Antennas Propag.*, vol. 70, no. 10, pp. 9918–9923, Oct. 2022.
- [112] F. Sun et al., "A millimeter-wave wideband dual-polarized antenna array with 3-D-printed air-filled differential feeding cavities," *IEEE Trans. Antennas Propag.*, vol. 70, no. 2, pp. 1020–1032, Feb. 2022.
- [113] K. K. So, K. M. Luk, C. H. Chan, and K. F. Chan, "3-D printed high gain complementary dipole/slot antenna array," *Appl. Sci.*, vol. 8, no. 8, p. 1410, 2018. [Online]. Available: <https://www.mdpi.com/2076-3417/8/8/1410>
- [114] C. Turkmen and M. Secmen, "Dual-band omnidirectional and circularly polarized slotted waveguide array antenna for satellite telemetry and telecommand," *IEEE Antennas Wireless Propag. Lett.*, vol. 20, no. 11, pp. 2100–2104, Nov. 2021.
- [115] M. F. Nakmouche, D. Deslandes, and G. Gagnon, "Machine learning aided design of sub-array MIMO antennas for CubeSats based on 3-D printed metallic ridge gap waveguides," in *Proc. IEEE Future Netw. World Forum (FNWF)*, 2022, pp. 418–421.
- [116] S. Wu, J. Li, Y. Cao, S. Yan, K. Xu, and H. Luyen, "Three-dimensional printed, dual-band, dual-circularly polarized antenna array using gap waveguide technology," *Appl. Sci.*, vol. 12, no. 21, 2022, Art. no. 10704. [Online]. Available: <https://www.mdpi.com/2076-3417/12/21/10704>
- [117] M. J. Rigby, T. Whitaker, and W. Whittow, "An anisotropic 3-D printed circular polarization converter for a patch antenna array operating in the Ka band," in *Proc. 16th Eur. Conf. Antennas Propag. (EuCAP)*, 2022, pp. 1–5.
- [118] F. Sun, Y. Li, L. Ge, and J. Wang, "Millimeter-wave magneto-electric dipole antenna array with a self-supporting geometry for time-saving metallic 3-D printing," *IEEE Trans. Antennas Propag.*, vol. 68, no. 12, pp. 7822–7832, Aug. 2020.
- [119] D. Pla et al., "High efficiency and circular polarization in SATCOM phased arrays using tri-ridge apertures," *Sci. Rep.*, vol. 14, no. 1, Aug. 2024, Art. no. 20285. [Online]. Available: <https://doi.org/10.1038/s41598-024-71085-z>
- [120] H. Oosthuizen, (Stellenbosch Univ., Stellenbosch, South Africa). *DMLS 3D-Printed Active Antenna Array*. Mar. 2020. [Online]. Available: <http://hdl.handle.net/10019.1/108100>
- [121] K. Hu, G. Soto-Valle, Y. Cui, and M. M. Tentzeris, "Flexible and scalable additively manufactured tile-based phased arrays for satellite communication and 50 mm wave applications," in *Proc. IEEE/MTT-S Int. Microw. Symp. (IMS)*, 2022, pp. 691–694.
- [122] H. I. A. EL-Sawaf. "Shared-aperture 3-D-printed dielectric resonator antenna arrays for millimeter-wave applications." 2020. [Online]. Available: <https://uwspace.uwaterloo.ca/items/fe997ef2-c8b8-4f20-bbd5-29aa2c6b424f>
- [123] S. Wu, J. Li, J. Yao, Y. Cao, Y. Li, and X. Zhang, "3-D-printed ka-band circularly-polarized monopulse antenna array with high gain and low axial ratio," *IEEE Trans. Antennas Propag.*, vol. 72, no. 11, pp. 8282–8293, Nov. 2024.
- [124] B. Peres, P. Lemaitre-Auger, F. Schwartz, and T. P. Vuong, "Monolithic additive manufacturing of a dual-mode cavity filter based on ellipsoidal resonators," in *Proc. 54th Eur. Microw. Conf. (EuMC)*, 2024, pp. 365–368.
- [125] P. Vaitukaitis, K. Nai, and J. Hong, "A versatile 3-D printable model for implementing multiband waveguide filters with flexible filtering characteristics," *IEEE Access*, vol. 11, pp. 110051–110059, 2023.
- [126] P. Vaitukaitis, K. Nai, and J. Hong, "Investigation of metal 3-D printed high- Q multiband waveguide filters using spherical resonators," *IEEE Access*, vol. 12, pp. 1497–1507, 2024.
- [127] P. Vaitukaitis, K. Nai, J. Rao, and J. Hong, "3-D metal printed deformed elliptical cavity bandpass filter with wide stopband," in *Proc. 51st Eur. Microw. Conf. (EuMC)*, 2022, pp. 704–707.
- [128] P. Vaitukaitis, K. Nai, J. Rao, and J. Hong, "On the development of metal 3-D printed bandpass filter with wide stopband based on deformed elliptical cavity resonator with an additional plate," *IEEE Access*, vol. 10, pp. 15427–15435, 2022.
- [129] P. Vaitukaitis, K. Nai, J. Rao, M. S. Bakr, and J. Hong, "Technological investigation of metal 3-D printed microwave cavity filters based on different topologies and materials," *IEEE Trans. Compon., Packag. Manuf. Technol.*, vol. 12, no. 12, pp. 2027–2037, Dec. 2022.
- [130] M. Baranowski, U. Balewski, A. Lamecki, and M. Mrozowski, "Fast design optimization of waveguide filters applying shape deformation techniques," in *Proc. 24th Int. Microw. Radar Conf. (MIKON)*, 2022, pp. 1–4.
- [131] M. Baranowski, u. Balewski, A. Lamecki, M. Mrozowski, and J. Galdeano, "A circular waveguide dual-mode filter with improved out-of-band performance for satellite communication systems," *IEEE Microw. Wireless Compon. Lett.*, vol. 32, no. 12, pp. 1403–1406, Dec. 2022.
- [132] M. Li, Y. Yang, F. Iacopi, M. Yamada, and J. Nulman, "Compact multilayer bandpass filter using low-temperature additively manufacturing solution," *IEEE Trans. Electron Devices*, vol. 68, no. 7, pp. 3163–3169, Jul. 2021.
- [133] O. A. Peverini et al., "Integration of an H-plane bend, a twist, and a filter in ku/K-band through additive manufacturing," *IEEE Trans. Microw. Theory Techn.*, vol. 66, no. 5, pp. 2210–2219, May 2018.
- [134] M. K. Moghaddam and R. Fleury, "Miniatirized metamaterial filters compatible with standard waveguide technology," in *Proc. 15th Int. Congr. Artif. Mater. Novel Wave Phenomena (Metamaterials)*, 2021, pp. 197–199.
- [135] M. Khatibi Moghaddam and R. Fleury, "Subwavelength metawaveguide filters and metaports," *Phys. Rev. Appl.*, vol. 16, no. 4, 2021, Art. no. 44010.
- [136] D. Santiago, M. A. G. Laso, T. Lopetegi, and I. Arregui, "Novel design method for millimeter-wave gap waveguide low-pass filters using advanced manufacturing techniques," *IEEE Access*, vol. 11, pp. 89711–89719, 2023.
- [137] X. Wen, Y. Yu, C. Tian, C. Guo, W. Wu, and F. Li, "An Invar alloy SLM printed diplexer with high thermal stability," *IEEE Trans. Circuits Syst. II, Exp. Briefs*, vol. 69, no. 3, pp. 1019–1023, Mar. 2022.
- [138] L. Polo-López et al., "Mechanically reconfigurable linear phased array antenna based on single-block waveguide reflective phase shifters with tuning screws," *IEEE Access*, vol. 8, pp. 113487–113497, 2020.
- [139] J. Melendro-Jiménez, P. Sanchez-Olivares, A. Tamayo-Domínguez, J. Luis Masa-Campos, and J.-M. Fernández-González, "A novel logarithmic-spiral-shaped 3-D-printed dielectric polarizer for dual-circularly polarized conical-beam radiation patterns in the Ka-band," *IEEE Trans. Antennas Propag.*, vol. 72, no. 8, pp. 6219–6228, 2024.
- [140] I. O. de Saracho Pantoja. "Ku band waveguide diplexer design for satellite communication. Implementation by additive manufacturing and experimental characterization." 2015. [Online]. Available: https://oa.upm.es/37345/1/PFC_IRENE_ORTIZ_DE_SARACHO_PANTOJA_2015.pdf
- [141] F. L. Borgne, G. Cochet, J. Haumont, D. Diedhiou, K. Donnart, and A. Manchec, "An integrated monobloc 3-D printed front-end in ku-band," in *Proc. 49th Eur. Microw. Conf. (EuMC)*, 2019, pp. 786–789.
- [142] E. Laplanche et al., "A ku-band diplexer based on 3-DB directional couplers made by plastic additive manufacturing," in *Proc. 47th Eur. Microw. Conf. (EuMC)*, 2017, pp. 428–431.
- [143] I. Agnihotri and S. K. Sharma, "Design of a compact 3-D metal printed Ka-band waveguide polarizer," *IEEE Antennas Wireless Propag. Lett.*, vol. 18, no. 12, pp. 2726–2730, Dec. 2019.
- [144] C. Molero, H. Legay, T. Pierré, and M. García-Vigueras, "Broadband 3-D-printed polarizer based on metallic transverse electro-magnetic unit-cells," *IEEE Trans. Antennas Propag.*, vol. 70, no. 6, pp. 4632–4644, Jun. 2022.
- [145] S. Khan, N. Vahabzani, and M. Daneshmand, "A fully 3-D printed waveguide and its application as microfluidically controlled waveguide switch," *IEEE Trans. Compon., Packag. Manuf. Technol.*, vol. 7, no. 1, pp. 70–80, Jan. 2017.



- [146] Y. Ushijima, H. Yukawa, T. Takahashi, and N. Yoneda, "K-band waveguide terminator suitable for additive manufacturing technology and its applications," in *Proc. 54th Eur. Microw. Conf. (EuMC)*, 2024, pp. 192–195.
- [147] J.-H. Cho, K.-Y. Park, C.-M. Lim, and H.-W. Son, "Design and implementation of an X-band horn antenna with a metamaterial lens using 3-D printing technology," *IEEE Access*, vol. 12, pp. 17773–17781, 2024.
- [148] "Tyndall equipment catalogue for advanced research and fabrication." 2025. [Online]. Available: <https://www.tyndall.ie/about-us/infrastructure/tyndall-equipment-catalogue/>
- [149] C. Labs, "How cold is outer space? Tritium batteries for space technology," Aug. 2023. [Online]. Available: <https://citylabs.net/cold-outer-space/>
- [150] E. A. Plis and G. Badura, "The spectral characterization of novel spacecraft materials in the low earth orbit environment," *J. Astronaut. Sci.*, vol. 71, no. 2, p. 15, Mar. 2024. [Online]. Available: <https://link.springer.com/10.1007/s40295-024-00436-9>
- [151] S. F. Xavier, *Thermoplastic Polymer Composites: Processing, Properties, Performance, Applications and Recyclability*. Hoboken, NJ, USA: Wiley, 2022.
- [152] X. Wang et al., "Research progress in polylactic acid processing for 3-D printing," *J. Manuf. Process.*, vol. 112, pp. 161–178, Feb. 2024. [Online]. Available: <https://www.sciencedirect.com/science/article/pii/S1526612524000483>
- [153] M. S. Razali et al., "Preparation and properties enhancement of poly (lactic acid)/calcined-seashell biocomposites for 3-D printing applications," *J. Appl. Polym. Sci.*, vol. 139, no. 5, 2022, Art. no. 51591.
- [154] Z. Yang, X. Feng, M. Xu, and D. Rodrigue, "Printability and properties of 3-D-printed poplar fiber/polylactic acid biocomposite," *BioResources*, vol. 16, no. 2, p. 2774, 2021.
- [155] A. Selvam, S. Mayilswamy, R. Whenish, R. Velu, and B. Subramanian, "Preparation and evaluation of the tensile characteristics of carbon fiber rod reinforced 3-D printed thermoplastic composites," *J. Composites Sci.*, vol. 5, no. 1, p. 8, 2021. [Online]. Available: <https://www.mdpi.com/2504-477X/1/8>
- [156] M. M. Silva, P. E. Lopes, Y. Li, P. Pötschke, F. N. Ferreira, and M. C. Paiva, "Polylactic acid/carbon nanoparticle composite filaments for sensing," *Appl. Sci.*, vol. 11, no. 6, p. 2580, 2021. [Online]. Available: <https://www.mdpi.com/2076-3417/11/6/2580>
- [157] D. Helena, A. Ramos, T. Varum, and J. N. Matos, "The use of 3-D printing technology for manufacturing metal antennas in the 5G/IoT context," *Sensors*, vol. 21, no. 10, p. 3321, 2021. [Online]. Available: <https://www.mdpi.com/1424-8220/21/10/3321>
- [158] E. Lobov, I. Vindokurov, and M. Tashkinov, "Mechanical properties and performance of 3-D-printed acrylonitrile butadiene styrene reinforced with carbon, glass and basalt short fibers," *Polymers*, vol. 16, no. 8, p. 1106, 2024. [Online]. Available: <https://www.mdpi.com/2073-4360/16/8/1106>
- [159] H. K. Sezer and O. Eren, "FDM 3-D printing of MWCNT re-inforced ABS nano-composite parts with enhanced mechanical and electrical properties," *J. Manuf. Process.*, vol. 37, pp. 339–347, Jan. 2019. [Online]. Available: <https://www.sciencedirect.com/science/article/pii/S1526612518318577>
- [160] A. Gao et al., "Highly conductive and light-weight acrylonitrile-butadiene-styrene copolymer/reduced graphene nanocomposites with segregated conductive structure," *Composites A Appl. Sci. Manuf.*, vol. 122, pp. 1–7, Jul. 2019. [Online]. Available: <https://www.sciencedirect.com/science/article/pii/S1359835X19301447>
- [161] Y. Wang, J. Shi, S. Lu, and W. Xiao, "Investigation of porosity and mechanical properties of graphene nanoplatelets-reinforced AlSi10 mg by selective laser melting," *J. Micro Nano-Manuf.*, vol. 6, no. 1, Dec. 2017, Art. no. 10902. [Online]. Available: https://asmedigitalcollection.asme.org/micronanomanufacturing/article-pdf/6/1/010902/5950730/jmmn_006_01_010902.pdf
- [162] S. W. Paek, S. Balasubramanian, and D. Stupples, "Composites additive manufacturing for space applications: A review," *Materials*, vol. 15, no. 13, p. 4709, 2022. [Online]. Available: <https://www.mdpi.com/1996-1944/15/13/4709>
- [163] A. Shastri et al., "3-D printing of millimetre wave and low-terahertz frequency selective surfaces using aerosol jet technology," *IEEE Access*, vol. 8, pp. 177341–177350, 2020.
- [164] R. Shivakumar et al., "POSS enhanced 3-D graphene-polyimide film for atomic oxygen endurance in low earth orbit space environment," *Polymer*, vol. 191, Mar. 2020, Art. no. 122270. [Online]. Available: <https://www.sciencedirect.com/science/article/pii/S0032386120301099>
- [165] Z.-Y. Zou et al., "Near-zero thermal expansion bal-SrZn₂Si₂O₇-based microwave dielectric ceramics for 3-D printed dielectric resonator antenna with integrative lens," *Adv. Mater. Interfaces*, vol. 8, no. 15, 2021, Art. no. 2100584. [Online]. Available: <https://onlinelibrary.wiley.com/doi/abs/10.1002/admi.202100584>
- [166] A. Fontana et al., "A novel approach toward the integration of fully 3-D printed surface-mounted microwave ceramic filters," *IEEE Trans. Microw. Theory Techn.*, vol. 71, no. 9, pp. 3915–3928, May 2023.
- [167] V. Nova et al., "3-D printed waveguide filters: Manufacturing process and surface mounted assembly," *IEEE Trans. Microw. Theory Techn.*, vol. 71, no. 12, pp. 5266–5279, Dec. 2023.
- [168] P. Colombo, G. Mera, R. Riedel, and G. D. Soraru, "Polymer-derived ceramics: 40 years of research and innovation in advanced ceramics," *J. Amer. Ceram. Soc.*, vol. 93, no. 7, pp. 1805–1837, 2010. [Online]. Available: <https://ceramics.onlinelibrary.wiley.com/doi/abs/10.1111/j.1551-2916.2010.03876.x>
- [169] R. Riedel, G. Mera, R. Hauser, and A. Klonczynski, "Silicon-based polymer-derived ceramics: Synthesis properties and applications—a review dedicated to prof. Dr. Fritz Aldinger on the occasion of his 65th birthday," *J. Ceram. Soc. Jpn.*, vol. 114, no. 1330, pp. 425–444, 2006.
- [170] R. Riedel, "Advanced ceramics from inorganic polymers," *Mater. Sci. Technol. A*, to be published.
- [171] D. Kopeliovich, "Advances in the manufacture of ceramic matrix composites using infiltration techniques," in *Proc. Adv. Ceramic Matrix Composites*, 2014, pp. 79–108.
- [172] Y. Lakhdar, C. Tuck, J. Binner, A. Terry, and R. Goodridge, "Additive manufacturing of advanced ceramic materials," *Progr. Mater. Sci.*, vol. 116, Feb. 2021, Art. no. 100736. [Online]. Available: <https://www.sciencedirect.com/science/article/pii/S0079642520301006>
- [173] Y. Kok et al., "Anisotropy and heterogeneity of microstructure and mechanical properties in metal additive manufacturing: A critical review," *Mater. Design*, vol. 139, pp. 565–586, Feb. 2018. [Online]. Available: <https://www.sciencedirect.com/science/article/pii/S0264127517310493>
- [174] W. J. Hwang, G. B. Bang, and S.-H. Choa, "Effect of a stress relief heat treatment of AlSi₇Mg and AlSi₁₀Mg alloys on mechanical and electrical properties according to silicon precipitation," *Met. Mater. Int.*, vol. 29, no. 5, pp. 1311–1322, May 2023.
- [175] B. Zhang et al., "Metallic 3-D printed antennas for millimeter- and submillimeter wave applications," *IEEE Trans. Terahertz Sci. Technol.*, vol. 6, no. 4, pp. 592–600, Jun. 2016.
- [176] S. Das and S. Das, "Properties for polymer, metal and ceramic based composite materials," in *Reference Module in Materials Science and Materials Engineering*. Faenza, Italy: Trans. Tech., Jan. 2021.
- [177] M. Pagac et al., "A review of vat photopolymerization technology: Materials, applications, challenges, and future trends of 3-D printing," *Polymers*, vol. 13, p. 598, Feb. 2021.
- [178] X. Zhu, B. Zhang, and K. Huang, "A λ -band dielectric and metallic 3-D printed aperture shared multibeam parabolic reflector antenna for satellite communication," *Int. J. RF Microw. Comput.-Aided Eng.*, vol. 30, no. 7, 2020, Art. no. e22216. [Online]. Available: <https://onlinelibrary.wiley.com/doi/abs/10.1002/mmce.22216>
- [179] M. Rimšauskas, E. Jasūniūnė, T. Kuncius, R. Rimšauskienė, and V. Cicénas, "Investigation of influence of printing parameters on the quality of 3-D printed composite structures," *Composite Struct.*, vol. 281, Feb. 2022, Art. no. 115061. [Online]. Available: <https://www.sciencedirect.com/science/article/pii/S0263822321014811>
- [180] C. Li and J. Qi, "Structural analysis of 3D printing model," in *Proc. 7th Int. Conf. Mechatron., Comput. Educ. Informationization (MCEI)*, 2017, pp. 289–293.
- [181] S. Manshari, S. Koziel, and L. Leifsson, "Compact dual-polarized corrugated horn antenna for satellite communications," *IEEE Trans. Antennas Propag.*, vol. 68, no. 7, pp. 5122–5129, Jul. 2020.
- [182] M. Gholami and M.-R. Nezhad-Ahmadi, "A wideband combined LNA-filter in 22 nm FD-SOI technology for satellite phased arrays," *Microw. Opt. Technol. Lett.*, vol. 66, no. 9, 2024, Art. no. e34338. [Online]. Available: <https://onlinelibrary.wiley.com/doi/abs/10.1002/mop.34338>

- [183] X. Li, X. Huang, S. Mathisen, R. Letizia, and C. Paoloni, "Design of 71–76 GHz double-corrugated waveguide Traveling-wave tube for satellite downlink," *IEEE Trans. Electron Devices*, vol. 65, no. 6, pp. 2195–2200, Jan. 2018.
- [184] Q. Nian et al., "Direct laser writing of nanodiamond films from graphite under ambient conditions," *Sci. Rep.*, vol. 4, no. 1, p. 6612, Oct. 2014. [Online]. Available: <https://doi.org/10.1038/srep06612>
- [185] M. Hogan, "What is additive manufacturing? The complete definition [2023]," Dec. 2022. [Online]. Available: <https://nexa3-D.com/blog/additive-manufacturing/>
- [186] O. A. Mohamed, "Analytical modeling and experimental investigation of product quality and mechanical properties in FDM additive manufacturing," Ph.D. dissertation, Dept. Mech., Swinburne Univ. Technol., Hawthorn, VIC, Australia, 2017.
- [187] R. Hensleigh et al., "Charge-programmed three-dimensional printing for multi-material electronic devices," *Nat. Electron.*, vol. 3, pp. 1–9, Apr. 2020.
- [188] R. Chaudhary, P. Fabbri, E. Leoni, F. Mazzanti, R. Akbari, and C. Antonini, "Additive manufacturing by digital light processing: A review," *Progr. Additive Manuf.*, vol. 8, no. 2, pp. 331–351, 2023.
- [189] C. R. Ocier et al., "Direct laser writing of volumetric gradient index lenses and waveguides," *Light Sci. Appl.*, vol. 9, no. 1, p. 196, 2020.
- [190] S. Raja, "The systematic development of direct write (DW) technology for the fabrication of printed antennas for the aerospace and defence industry," Ph.D. dissertation, Mech. Elect. Manuf. Eng., Loughborough Univ., Loughborough, U.K., 2014.
- [191] T. Blachowicz, G. Ehrmann, and A. Ehrmann, "Metal additive manufacturing for satellites and rockets," *Appl. Sci.*, vol. 11, no. 24, 2021, Art. no. 12036.
- [192] P. Martín-Iglesias et al., "Metal 3-D printing for RF/microwave high-frequency parts," *CEAS Space J.*, vol. 15, no. 1, pp. 7–25, 2023.
- [193] V. Basile et al., "Design and manufacturing of super-shaped dielectric resonator antennas for 5G applications using stereolithography," *IEEE Access*, vol. 8, pp. 82929–82937, 2020.
- [194] H. Yang, G. Tsiklos, R. Ronaldo, and S. Ratchev, "Application of microstereolithography technology in micromanufacturing," in *Proc. Int. Micro-Assem. Technol. IFIP TC5 WG5*, 2008, pp. 171–176.
- [195] J. Wang, Z. Xu, Z. Wang, X. Zheng, and Y. Rahmat-Samii, "Development of a low-cost lightweight advanced K-band horn antenna with charge-programmed deposition 3-D printing," *IEEE Antennas Wireless Propag. Lett.*, vol. 22, no. 8, pp. 1917–1921, Aug. 2023.
- [196] H. Zhang, Y. Qian, G. Wang, and Q. Zheng, "The characteristics of arc beam shaping in hybrid plasma and laser deposition manufacturing," *Sci. China E*, vol. 49, pp. 238–247, Mar. 2006.
- [197] F. H. Liu, Y. S. Liao, and H. P. Wang, "Formability of the layer additive ceramic part," in *Materials Sciences Forum*, vol. 594. Faenza, Italy: Trans. Tech., 2008, pp. 241–248.
- [198] J. Zhou et al., "In-situ laser surface remelting of laser powder bed fused AlSi10Mg alloy at argon and nitrogen protective gases: Multiscale analysis," *Opt. Laser Technol.*, vol. 181, no. 3, 2025, Art. no. 111631.
- [199] J. Yang, X. Ma, K. Lin, X. Zhou, J. Zhu, and X. Tian, "A prospective study of 3-D printed continuous fiber reinforced composites in satellite antennas," in *Proc. 6th Int. Conf. Optoelectron. Sci. Mater. (ICOSM)*, vol. 134460, 2024, pp. 125–139.
- [200] Y. Cheng and Y. Dong, "3-D-printed high-gain millimeter-wave horn antenna with a hybrid metal and dielectric lens," *IEEE Trans. Antennas Propag.*, vol. 73, no. 2, pp. 830–839, Feb. 2025.
- [201] L. Wang et al., "Current advances and future perspectives of MXene-based electromagnetic interference shielding materials," *Adv. Composites Hybrid Mater.*, vol. 6, no. 5, p. 172, Sep. 2023. [Online]. Available: <https://doi.org/10.1007/s42114-023-00752-y>
- [202] M. Han et al., "Solution-processed Ti_3C_2Tx MXene antennas for radio-frequency communication," *Adv. Mater.*, vol. 33, no. 1, Jan. 2021, Art. no. 2003225. [Online]. Available: <https://onlinelibrary.wiley.com/doi/10.1002/adma.202003225>
- [203] V. Karimi and V. E. Babicheva, "MXene-antenna electrode with collective multipole resonances," *Nanoscale*, vol. 16, no. 9, pp. 4656–4667, 2024. [Online]. Available: <https://xlink.rsc.org/?DOI=D3NR03828A>
- [204] R. Colella et al., "Electromagnetic characterisation of conductive 3-D-printable filaments for designing fully 3-D-printed antennas," *IET Microw. Antennas Propag.*, vol. 16, no. 11, pp. 687–698, 2022. [Online]. Available: <https://ietresearch.onlinelibrary.wiley.com/doi/abs/10.1049/mia2.12278>
- [205] U. Hasni, R. Green, A. V. Filippas, and E. Topsakal, "One-step 3-D-printing process for microwave patch antenna via conductive and dielectric filaments," *Microw. Opt. Technol. Lett.*, vol. 61, no. 3, pp. 734–740, 2019. [Online]. Available: <https://onlinelibrary.wiley.com/doi/abs/10.1002/mop.31607>
- [206] Z. Lyu, J. Wang, and Y. Chen, "4D printing: Interdisciplinary integration of smart materials, structural design, and new functionality," *Int. J. Extreme Manuf.*, vol. 5, no. 3, Sep. 2023, Art. no. 32011. [Online]. Available: <https://iopscience.iop.org/article/10.1088/2631-7990/ace090>
- [207] Z. Wang, B. Zhang, and K. Huang, "A metallic 3-D printed K -band quasi-pyramidal-horn antenna array," *Int. J. RF Microw. Comput.-Aided Eng.*, vol. 30, no. 7, p. 19, Jul. 2020. [Online]. Available: <https://onlinelibrary.wiley.com/doi/10.1002/mmce.22217>
- [208] "NASA technical standards—Standards." 2010. [Online]. Available: <https://standards.nasa.gov/NASA-Technical-Standards>



HAFSA TALPUR (Member, IEEE) received the B.Eng. degree in telecommunication engineering and the M.Eng. degree in computer information engineering from the Mehran University of Engineering and Technology, Pakistan, in 2021 and 2024, respectively. She is currently pursuing the Ph.D. degree with the SIGCOM Research Group, Interdisciplinary Centre for Security, Reliability, and Trust, University of Luxembourg. From 2022 to 2024, she remained a Research Associate with the Antenna Measurement and Testing Laboratory, Department of Telecommunication Engineering, Mehran University of Engineering and Technology, Pakistan. She has achieved outstanding recognition award for her exceptional work at that position. Since 2024, During her M.Eng. she published three conference articles and a book chapter. Her current research interests include antennas, RF components, meta-surfaces, beam-forming networks and additive manufacturing processes for onboard antennas and user terminals. She is an active IEEE and Microwave Theory and Techniques Society Member.



ULAN MYRZAKHAN (Member, IEEE) received the B.S. degree in electrical and electronics engineering from Nazarbayev University, Astana, Kazakhstan, in 2017, and the M.S. and Ph.D. degrees in electrical and computer engineering from the King Abdullah University of Science and Technology, Thuwal, Saudi Arabia, in 2019 and 2024, respectively. He is currently a Research Associate with the Interdisciplinary Centre for Security, Reliability, and Trust, University of Luxembourg. His research interests include the design and development of antennas and antenna systems for satellite onboard applications and user terminals, with a focus on utilizing cost-effective additive manufacturing techniques for fabrication.



JUAN ANDRES VÁSQUEZ-PERALVO (Member IEEE) was born in Quito, Ecuador. He received the his Bachelor of Engineering degree in electronics and telecommunications from the Escuela Politécnica Nacional, Quito, the Master of Science degree in wireless communication systems from the University of Sheffield, Sheffield, U.K., and the Ph.D. degree in communication systems from the Universidad Politécnica de Madrid, Madrid, Spain, in 2022. During his doctoral studies, he was a Research Visitor with the Illinois

Institute of Technology, Chicago, USA, supervised by Prof. T. Wong. He is currently a Research Scientist with the Université du Luxembourg, specializing in antenna design for satellite communications. His research interests include phased array systems, digital beamforming, additive manufacturing for onboard antennas and user terminals, meta-surfaces, vehicle antennas, and lens antenna design.



SYMEON CHATZINOTAS (Fellow, IEEE) received the M.Eng. degree in telecommunications from the Aristotle University of Thessaloniki, Thessaloniki, Greece, in 2003, and the M.Sc. and Ph.D. degrees in electronic engineering from the University of Surrey, Guildford, U.K., in 2006 and 2009, respectively. He is currently a Full Professor and the Deputy Head of the SIGCOM Research Group, Interdisciplinary Centre for Security, Reliability, and Trust, University of Luxembourg, Esch-sur-Alzette, Luxembourg, and a Visiting Professor

with the University of Parma, Parma, Italy. He has been involved in numerous research and development projects with the Institute of Informatics Telecommunications, National Center for Scientific Research Demokritos, Institute of Telematics and Informatics, Center of Research and Technology Hellas, and Mobile Communications Research Group, Center of Communication Systems Research, University of Surrey. He has co-authored more than 400 technical papers in refereed international journals, conferences and scientific books. His research interests include multiuser information theory, cooperative/cognitive communications, and wireless network optimization. He was the co-recipient of the 2014 IEEE Distinguished Contributions to Satellite Communications Award, the CROWNCOM 2015 Best Paper Award, and the 2018 EURASIP JWCN Best Paper Award. He is currently on the editorial board of the IEEE OPEN JOURNAL OF VEHICULAR TECHNOLOGY and the *International Journal of Satellite Communications and Networking*.



SHUAI ZHANG (Fellow, IEEE) received the B.E. degree from the University of Electronic Science and Technology of China, Chengdu, China, in 2007, and the Ph.D. degree in electromagnetic engineering from the Royal Institute of Technology (KTH), Stockholm, Sweden, in 2013. In 2014, he joined Aalborg University, Denmark, where he is currently a Full Professor and the Head of Antenna Research Group. In 2010 and 2011, he was a Visiting Researcher with Lund University, Sweden, and also with Sony Mobile

Communications AB, Sweden, respectively. He was also an External Antenna Specialist with Bang & Olufsen, Denmark, from 2016 to 2017. He has supervised/co-supervised ten Postdocs and 18 Ph.D. students. He has coauthored over 140 articles in well-reputed international journals and over 17 U.S. or WO patents. His citations in Scopus are over 6000 with H index of 39. His current research interests include: millimeter-wave antennas for cellular communications, bio-electromagnetics, metasurfaces, CubeSat antennas, massive MIMO antennas, wireless sensors, and RFID antennas. He is the recipient of “IEEE Antennas and Propagation Society Young Professional Ambassador” in 2022, where he gives presentation for different IEEE Chapters on Antennas for Mobile Communications. He is an Associate Editor of IEEE ANTENNAS AND WIRELESS PROPAGATION LETTERS and IET Microwaves, Antennas and Propagation. He is the General Co-Chair for iWAT2023 at Aalborg, Denmark, and the TPC or a meta reviewer for several top IEEE conferences. He has also been intensively invited to international conference and industry to give keynote/plenary speech and presentations. Since 2024, he has been the European Association on Antennas and Propagation Regional Delegate.